Structures 33 (2021) 4871–4894

Contents lists available at ScienceDirect

Structures

journal homepage: www.elsevier.com/locate/structures

Sizing optimization of truss structures using the political optimizer (PO) algorithm

Rafiq Awad

Department of Mechanical Engineering, University of Benghazi (UOB), Benghazi, Libya

ARTICLE INFO

Keywords:
Political optimizer
Truss optimization
Structural design
Continuous variable optimization
Metaheuristic algorithms

ABSTRACT

The challenge that structural optimization tasks pose by dint of their highly non-linear design constraints and complex solution domains has spurred both the implementation and development of many novel metaheuristic algorithms over the past two decades. In this study, the very recently proposed political optimizer algorithm has been implemented in the context of structural optimization. Inspired by the multi-phased political process in parliamentary democracies, the algorithm efficiently balances between exploration and exploitation by logically dividing the population of search agents into political parties that compete for constituency (electoral district) domination. This competitive-based population partitioning scheme ensures that enough of the search space is thoroughly investigated for the global optima all the while maintaining algorithmic speed and efficiency. Moreover, a local search mechanism known as the recent past-based position updating strategy (RPPUS) provides for an effective exploitation strategy where every search agent is allowed to learn from its previous behavior and hence collectively guide the population towards better solutions and away from worse ones. To quantitatively assess the performance of the algorithm, three planar trusses (10 bar, 18 bar, and 200 bar) and four space trusses (22 bar, 25 bar, 72 bar, and 942-bar) with multiple loading conditions and design constraints have been considered. Results show that for small/medium-scale structural systems, the PO algorithm outperforms all previously proposed state-of-the-art optimization methodologies in all aspects may it be final optimized weight, algorithmic stability, or convergence speeds, and that for larger structures excellent performance is still maintained but a certain, yet acceptable, extent of algorithmic instability is manifest. Based off these findings, future research into the PO algorithm as an efficient structural optimizer is strongly recommended.

1. Introduction

The ubiquity of truss structural systems in modern society has made the field of structural optimization an important engineering endeavor over the last couple of decades. The idea of designing structurally reliable, sustainable, and cost-effective trusses has largely been the impetus for the early development of many of the conventional, deterministic-based optimization methodologies that have long been employed in the field. Over the past two decades, however, the promise of metaheuristic techniques, which sacrifice solution quality for computational speed, as an alternative optimization methodology, has allured many structural engineers into the prospect of applying these new-found techniques to various structural design tasks. By its very nature, structural optimization problems are computationally costly due to the resulting force–displacement equations that require solving for every computational iteration. The problem is only compounded when real-world structures are to be addressed and the number of structural members along with the resulting degrees of freedom for every node have to be taken into consideration in the resulting stiffness matrix. For this reason, metaheuristic algorithms that are able to solve truss problems in fewer structural analyses are more desirable and are often sought after.

Owing to the No Free Lunch (NFL) theorem [1], which states that no single metaheuristic optimizer is well suited for all classes of optimization problems, structural engineers have sought to leverage this fact by implementing various algorithms in an attempt to find better methods to tackle structural design problems. The theorem recommends recognizing optimization problems as distinct classes of optimization tasks and then subsequently implement/develop optimization algorithms to perform effectively with respect to them. With that in mind, a number of techniques have been tested for efficiency of solution. Rajeev and Krishnamoorthy [2], for instance, adopted the Genetic Algorithm (GA) technique to optimize member sizes of trusses with discrete design variables. A similar GA approach was used by Cao [3] for the size optimization of skeletal structures with continuous variables. Fourie and Groenwold [4], Schutte and Groenwold [5], and

E-mail address: rafiq.bodalal@uob.edu.ly.

https://doi.org/10.1016/j.istruc.2021.07.027
Received 26 February 2021; Received in revised form 28 June 2021; Accepted 7 July 2021
Available online 17 August 2021
2352-0124/

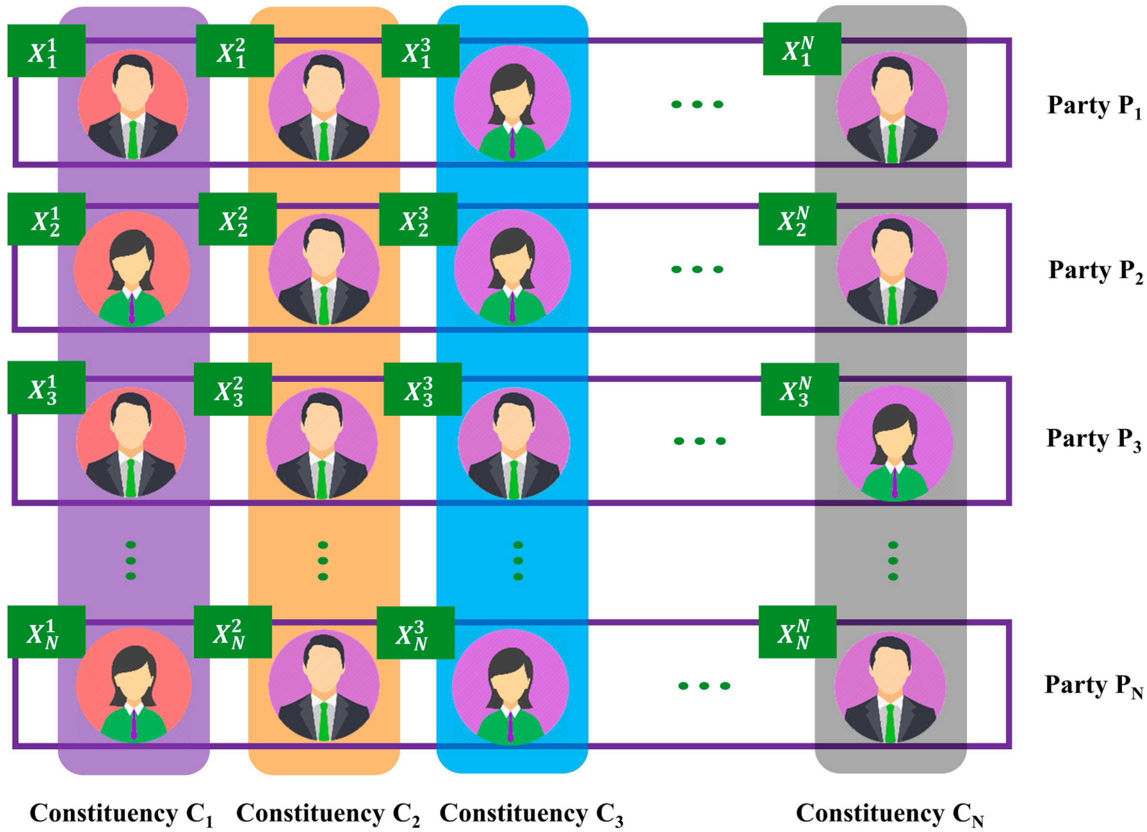

Fig. 1. A schematic of the population partitioning scheme into political parties and constituencies for the PO algorithm (party members with red backgrounds represent party leaders).

Li *et al.* [6] successfully applied the Particle Swarm Optimizer (PSO) technique for the size and layout optimization of structures in both discrete and continuous domains. Camp and Bichon used the Ant Colony Optimizer (ACO) to arrive at optimized structural weights with stress and displacement constraints [7]. Sonmez successfully optimized trusses using the Artificial Bee Colony (ABC) metaheuristic with continuous and discrete structural sizing members [8,9]. Lee and Geem investigated the efficiency of the Harmony Search (HS) algorithm in the context of structural optimization. Results were compared with those previously presented in literature and the HS method was proven to be effective at reducing truss weight under multiple loading conditions [10]. The Big Bang-Big Crunch (BB-BC) algorithm [11], which draws its inspiration from cosmology, was implemented for three-dimensional structural design problems by Camp [12]. Talatahari *et al.* employed the Firefly Algorithm (FA), developed by Yang [13], for determining the optimum design of tower structures using continuous sizing variables [14]. Degertekin and Hayalioglu [15] recognized the potential use of the Teaching-Learning based optimizer (TLBO) developed by Rao *et al.* [16] and applied it to the size optimization of structural systems with continuous variables. A similar attempt was made by Kaveh and Mahdavi [17] to ascertain the efficacy of the Colliding Bodies Optimizer (CBO) in structural design problems. In accordance with literature and research trend, Bekdas, *et al.* [18] investigated the robustness and versatility of the Flower Pollination Algorithm (FPA) developed by Yang [19] for its utilization in truss optimization. More recently, Kaveh and Bakshoopri [20] and Kooshkbaghi and Kaveh [21] introduced the novel Water Evaporation Optimizer (WEO) and Artificial Coronary Circulation Systems (ACCS) algorithms, respectively, to be specifically employed for structural design problems. This, ultimately, has spurred metaheuristic implementation beyond truss optimization and into moment and frame design under multiple loading and design constraints [22–24].

Researchers seeking to attain better results and algorithmic performance would often make inferences on specific metaheuristic aspects based on their implementation. Recognizing this fact, Kaveh [25] summarizes the results of 23 metaheuristic algorithms, specifically developed to tackle structural optimization problems, that have either been modified or implemented to serve as a reference for any new structural engineer embarking on truss design tasks. The book, at the end of each chapter, makes a number of recommendations and lists the effective exploitative/exploration tactics that may help in the development of newer optimization schemes. Using the information gained from metaheuristic implementations, many newer and more efficient structural optimization schemes have been developed. Prime examples of these modified algorithms include the Hybrid Big Bang-Big Crunch (HBB-BC) algorithm developed by Kaveh *et al.* [26] in attempt to overcome the inadequacies confronted by Camp [12], the modified TLBO (mTLBO) structural optimizer which came after the TLBO implementation [27], the Hybrid Particle Swarm-Swallow Swarm Optimization (HPSSO) algorithm that builds off the key results from the structural implementation of PSO and the Swallow Swarm Optimizer (SSO) [28], the Enhanced Bat Algorithm (EBA) [29], which improves the exploitative behavior of the BA algorithm, developed for the discrete and continuous sizing optimization of skeletal structures, the Accelerated Multi-Gravitational Search Algorithm (AMGSA) which is an improvement over the Gravitational Search Algorithm (GSA) in truss optimization [30], and the Enhanced Crow Search Algorithm (ECSA) [31] based off the CSA technique. A glance at literature trend points to the fact that the implementation of newer metaheuristics in structural design often opens up new avenues for potential research and development in the field.

Recently, a novel human behavior-based metaheuristic known as the Political Optimizer (PO) algorithm was developed by Askari *et al.* [32]. The algorithm's heuristic approach draws its inspiration from the social interactions that take place in politics. Search agents are logically divided into political parties and constituencies (electoral districts). Every member of which operates as a political party member that seeks

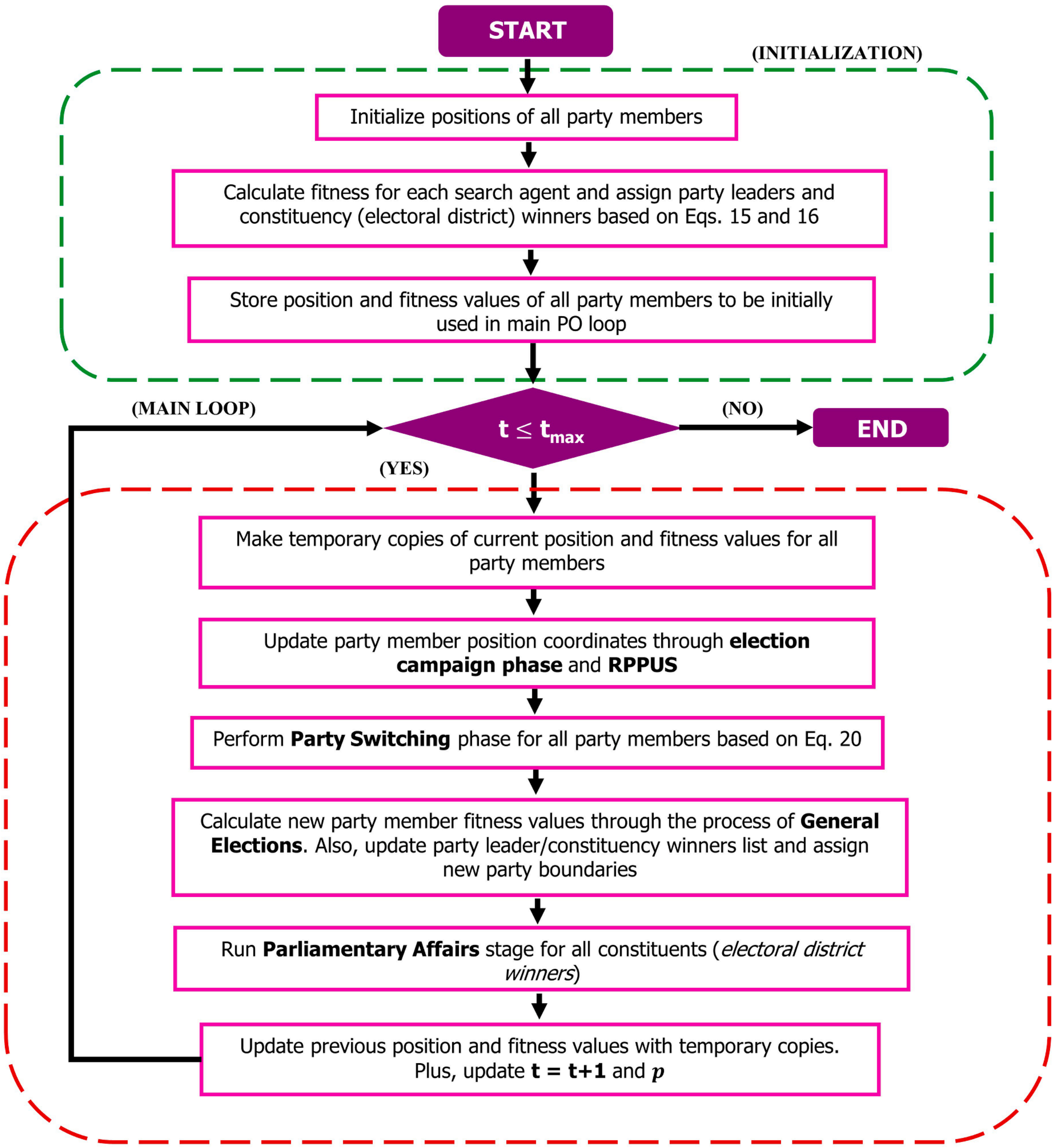

Fig. 2. Flowchart of the PO algorithm.

to maximize its fitness value by interacting with their local party leaders and constituency winners. The algorithm's well-established robust exploitation-exploration capabilities as well as its few performance parameters has convinced us to implement the PO technique to the structural sizing problem. Askari *et al.* [32] presented a comprehensive investigation into the efficacy of the proposed technique with 50 unimodal, multimodal, and fixed functions against 15 well-known metaheuristics. He furthermore tested the algorithm in a number of practical engineering applications such as gear train, spring and welded cantilever design problem. The results from the study proved the wide-scale effectiveness of the PO algorithm in a number of optimization problems in terms of algorithmic stability, convergence speeds, and optimized solutions. This has prompted multiple studies to be carried out to implement the novel technique in a number of other practical engineering applications [33–35] and showcase the competitive efficiency of the algorithm at arriving at optimal solutions.

In this study, the robustness and versatility of the novel political optimizer (PO) algorithm is applied to the problem of sizing optimization of truss structures. A total of seven structural systems, in both planar and spatial domains, with continuous design variables and multiple loading conditions were employed as benchmarks. To the best of the author's knowledge, no attempt has been made in literature to quantitatively evaluate the algorithm's performance in structural design so far. In accordance with previous studies, the comparison methodology adopted is by comparing final results with those obtained by previously mentioned metaheuristics published in literature.

The remainder of this work is organized as follows: Section 2 presents the formulation of the structural optimization task. Section 3 discusses the philosophical inspiration behind the development of the political optimizer technique as well as the pseudocode of the algorithm in detail. The formal analysis and findings of the PO algorithm's effectiveness in comparison with other metaheuristic methods is presented in Section 4 using seven classic structural benchmark problems. Section 5 summarizes the discussion and findings from the structural

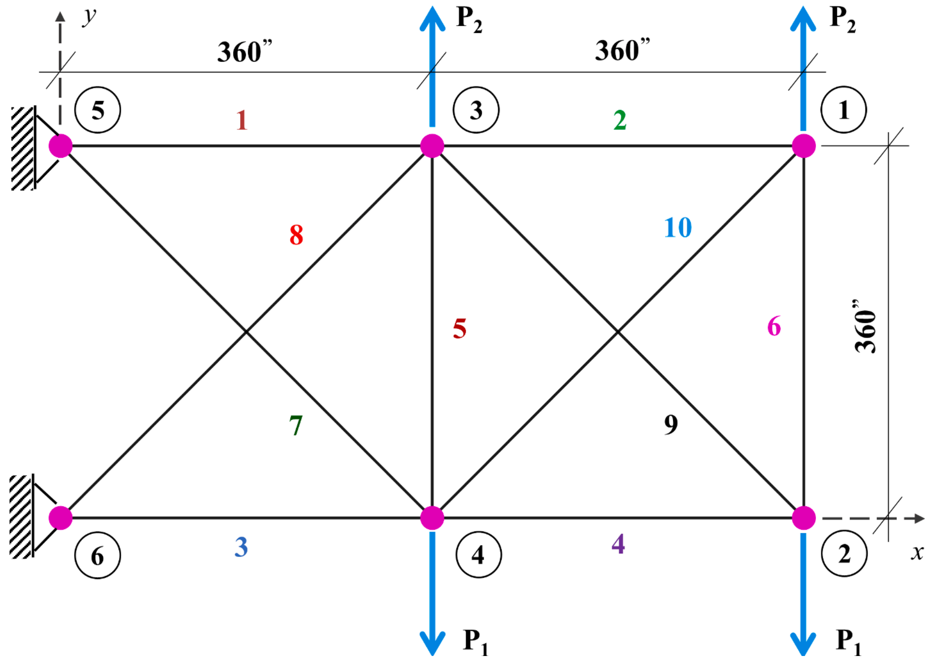

Fig. 3. Schematic of the 10-bar planar truss structure.

Table 1
Tabulated sensitivity results of the parameter N on PO algorithm performance ($\lambda = 0.5$).

N	Weight (Ib.)			
	Best	Worst	Mean	Standard Deviation
2	6070.94	9807.36	7889.58	832.22
3	5302.79	7930.88	6467.13	604.22
4	5065.77	6675.95	5644.51	432.62
5	5061.79	5728.76	5151.16	138.48
6	5061.12	5158.22	5078.625	16.545
7	5060.99	5100.34	5075.43	15.34
8	5060.94	5087.38	5069.00	8.59
9	5060.92	5083.25	5067.72	3.91
10	5060.88	5073.48	5065.51	1.26
11	**5060.85**	**5069.54**	**5061.23**	**0.53**
12	5061.34	5078.09	5065.22	3.085
13	5062.90	5079.38	5066.12	7.21
14	5063.95	5080.21	5067.47	9.31
15	5066.31	5082.23	5068.37	11.89

Note: 1 Ib. = 4.45 N.

Table 2
Tabulated sensitivity results of the parameter λ on PO algorithm performance ($N = 8$).

λ	**Weight (Ib.)**			
	Best	**Worst**	**Mean**	**Standard Deviation**
0.1	5060.86	5079.12	5065.67	9.42
0.2	5060.87	5082.72	5067.42	9.14
0.3	5060.87	5089.08	5068.57	8.5
0.4	5060.85	5087.74	5067.61	7.6
0.5	**5060.86**	**5081.10**	**5066.21**	**5.8**
0.6	5060.88	5208.46	5070.86	8.49
0.7	5060.89	5092.37	5071.97	12.82
0.8	5060.87	5082.21	5068.76	13.214
0.9	5060.94	5087.98	5069.29	18.62
1.0	5060.98	5082.38	5067.86	28.3
1.1	5060.92	5181.89	5071.09	47.90

Note: 1 Ib. = 4.45 N.

implementation section. Finally, Section 6 presents the conclusions and future recommendations based off the results of the study.

2. Problem formulation

The methodology of the present work is to minimize total structural weight by adopting the technique of a combined relaxed penalized objective function formulation and structural analysis of trusses. The latter being carried out by the *direct stiffness method* of analysis. Optimizing structural systems, in general, involves arriving at suitable member cross-sectional areas such that total structural weight is kept at a minimum all the while structural integrity (stress) and stiffness (nodal deflection) remain uncompromised. Mathematically, this expressed as

$$minimize\ W = \rho\sum_{i=1}^{nE} \mathrm{L}_i A_i, \qquad (\mathrm{A}_i \in \mathbb{R}) \tag{1}$$

with design variables

$$x = \{A_1, A_2, A_3, \cdots, A_{nG}\} \tag{2}$$

where W is the total truss weight, *nE* is the number of structural elements, *nG* is the number of design variables, ρ is the mass density of the structural material, L_i is the length of the *ith* member, A_i is the cross-sectional area of the *ith* member, and σ_i, $\sigma_i^b$and δ_j represent the normal stress, buckling stress and nodal displacement of the *ith* member and *jth* node, respectively.

Since most metaheuristic methods were originally developed to solve unconstrained optimization tasks, it is first necessary to convert the present design problem into an unconstrained one. In this study, a normalized constraint handling methodology is adopted where stress/displacement values for every structural member and node are compared with the maximum allowable stress, displacement, and buckling limits. The modified structural constraints are hence written as:

$$g_i^\sigma(x) = \frac{|\sigma_i(x)| - \sigma_{max}}{\sigma_{max}} \leq 0 \qquad i = 1, 2, 3 \cdots nE \tag{4}$$

$$g_j^\delta(x) = \frac{|\delta_j(x)| - \delta_{max}}{\delta_{max}} \leq 0 \qquad j = 1, 2, 3 \cdots nN \tag{5}$$

Table 3
Optimized results for the 10-bar planar truss (Case 1).

Design variable (in^2)	Li *et al.* [6] (HPSO)	Sonmez [8] (ABC-AP)	Degertekin [37] (EHS)	(SAHS)	Degertekin [15] (TLBO)	Kaveh *et al.* [38] MCSS	IMCSS	Kaveh & Bakhshpoori [20] (WEO)	Kaveh & Zolghadr [39] (CPA)	Javidi *et al.* [31] (CSA)	(ECSA)	Kooshkbaghi & Kaveh [21] (ACCS)	This study (PO)
A_1	30.704	30.548	30.208	30.394	30.4286	29.5766	30.0258	30.5755	30.5022	33.6116	30.5096	30.646	30.501
A_2	0.100	0.100	0.100	0.100	0.1000	0.1142	0.1	0.1000	0.1000	0.1478	0.1000	0.1	0.1
A_3	23.167	23.180	22.698	23.098	23.2436	23.8061	23.6277	23.3368	23.2170	22.9345	23.2253	23.103	23.198
A_4	15.183	15.218	15.275	15.491	15.3677	15.8875	15.9734	15.1497	15.2204	13.9637	15.2315	15.063	15.247
A_5	0.100	0.100	0.100	0.100	0.1000	0.1137	0.1	0.1000	0.1001	0.1050	0.1000	0.1	0.1
A_6	0.551	0.551	0.529	0.529	0.5751	0.1003	0.5167	0.5276	0.5587	0.3611	0.5517	0.573	0.55511
A_7	7.460	7.463	7.558	7.488	7.4404	8.6049	7.4567	7.4458	7.4548	7.9202	7.4561	7.478	7.4562
A_8	20.978	21.058	21.559	21.189	20.9665	21.6823	21.4374	20.9892	21.0371	22.0883	21.0276	21.094	21.035
A_9	21.508	21.501	21.491	21.342	21.5330	20.3033	20.7443	21.5236	21.5295	19.6785	21.5239	21.532	21.526
A_{10}	0.100	0.100	0.100	0.100	0.1000	0.1117	0.1	0.1000	0.1002	0.1041	0.1000	0.1	0.1
Weight (lb)	**5060.92**	**5060.880**	**5062.39**	**5061.42**	**5060.96**	**5086.9**	**5064.6**	**5060.99**	**5060.92**	**5095.40**	**5060.91**	**5061.03**	**5060.85**
Mean (lb)	N/A	N/A	5063.73	5061.95	5062.08	N/A	N/A	5062.09	5062.45	5290.79	5063.41	5061.07	5061.23
Stdev (lb)	N/A	N/A	1.98	0.71	0.79	N/A	N/A	2.05	3.77	125.89	5.43	0.09	0.53
CV (–)	None	None	None	None	None	None	None	None	None	None	None	None	None
NSA	125,000	500,000	9,791	7,081	16,872	8,875	8,475	19,540	23,700	18,706	16,401	12,000	7,920

Note: 1 in^2 = 6.452 cm^2; 1 lb. = 4.45 N.

$$g_k^b(x) = \frac{|\sigma_k^b(x)| - \sigma_{max}^b}{\sigma_{max}^b} \le 0 \qquad k = 1, 2, 3 \cdots nC \tag{6}$$

where $g_i^\sigma(x)$ is the normalized normal stress constraint for the *ith* member, σ_{max} is the maximum allowable normal stress limit for both tension and compression, $g_j^\delta(x)$ is the normalized displacement constraint for the jth node, δ_{max} is the maximum permissible nodal displacement value, $g_k^b(x)$ is the normalized buckling constraint for *kth* member in compression, σ_{max}^b is the critical buckling stress value when failure occurs, *nN* is the number of nodes in the truss, and *nC* is the number of structural members in compression.

Constraint values are governed by the following relation

$$if\ g_i(x) > 0\ then\ c_i = g_i(x) \tag{7}$$

$$elseif\ g_i(x) \le 0\ then\ c_i = 0 \tag{8}$$

The total constraint violation value for a single truss design is computed by summing all normalized stress and displacement penalty values for every truss member and node which is represented by a single variable as

$$C = \sum_{i=1}^{m} c_i = \sum_{i=1}^{nE}\left(\frac{|\sigma_i(x)| - \sigma_{max}}{\sigma_{max}}\right) + \sum_{j=1}^{nN}\left(\frac{|\delta_j(x)| - \delta_{max}}{\delta_{max}}\right) + \sum_{k=1}^{nC}\left(\frac{|\sigma_k^b| - \sigma_{max}^b}{\sigma_{max}^b}\right) \tag{9}$$

where m is the total number of evaluated constraints.

The final form of the penalized objective function sought to be minimized is thus

$$\psi(x) = \left(\rho \sum_{i=1}^{nE} \mathrm{L}_i \mathrm{A}_i\right) * Z * (1 + C)^{\epsilon} \tag{10}$$

where the variables Z and ϵ in Eq. 10 are the penalty scaling factor and penalty exponent, respectively, the value of which depends on problem size and complexity. Throughout this study, scaling factors have been taken as 1, for both Z and ϵ, as part of the relaxed objective function scheme [36]. Low penalization factors will facilitate the algorithm's explorative aspect and result in rapid convergence to global optimum structural designs. The value of the penalized objective function, therefore, is the product of the weight of a particular truss design and its total constraint/penalty violation which indirectly incorporates member stresses and nodal displacement values.

3. Political optimizer (PO)

3.1. Conceptual inspiration

The political optimizer (PO) algorithm is a recently developed human behavior-based metaheuristic which mathematically models all the major phases of democratic parliamentary politics. Phases such as party formation, electoral district allocation, party member swapping, election campaigning, inter-party elections, and parliamentary affairs are all included in the inner working of the algorithm. The central theme of democratic politics is based on the notion of populace representation in which political parties form the basic unit as well as the vehicle for various public outlooks to be represented in parliament. The objective of these parties is to maximize its number of parliamentary seats by competing with other parties through the process of inter-party elections and election campaigning in order to influence future government practices and policies. Party leaders assign party candidates that run for electoral districts (constituencies) in a bid to achieve parliament majority. In that regard, it can be said that for every constituency that is still contested, at least one party member from every party runs on its behalf. The goal of any party candidate, therefore, is to successfully run an

Table 4
Optimized results for the 10-bar planar truss (Case 2).

Design variable (in^2)	Li *et al.* [6] (HPSO)	Sonmez [8] (ABC-AP)	Degertekin [37]		Degertekin [15] (TLBO)	Kaveh & Bakhshpoori [20] (WEO)	Kaveh & Zolghadr [39] (CPA)	Khatibinia & Yazdani [30]		Kooshkbaghi & Kaveh [21] (ACCS)	Kaveh *et al.* [40] (PGO)	This study (PO)
			(EHS)	(SAHS)				(MGSA)	(AMGSA)			
A_1	23.353	23.4692	23.589	23.525	23.524	23.5804	23.5515	23.6	23.5	23.522	23.5326	23.62
A_2	0.100	0.1005	0.100	0.100	0.1000	0.1003	0.1000	0.1	0.1	0.1	0.1000	0.1
A_3	25.502	25.2393	25.422	25.429	25.441	25.1582	25.5440	25.4	25.4	25.364	25.0068	25.434
A_4	14.250	14.354	14.488	14.488	14.479	14.1801	14.1674	14.2	14.3	14.503	14.4241	14.351
A_5	0.100	0.1001	0.100	0.100	0.1000	0.1002	0.1000	0.1	0.1	0.1	0.1000	0.10003
A_6	1.972	1.9701	1.975	1.992	1.995	1.9708	1.9698	2.0	2.0	1.97	1.9721	1.9701
A_7	12.363	12.4128	12.362	12.352	12.334	12.4511	12.3533	12.4	12.4	12.417	12.4286	12.339
A_8	12.984	12.8925	12.682	12.698	12.689	12.9349	12.8167	12.8	12.8	12.938	12.8215	12.712
A_9	20.356	20.3343	20.322	20.341	20.354	20.3595	20.3302	20.5	20.3	20.058	20.4603	20.346
A_{10}	0.1010	0.1000	0.100	0.100	0.1000	0.1001	0.1001	0.1	0.1	0.1	0.1000	0.1
Weight (Ib)	**4677.29**	**4677.077**	**4679.02**	**4678.84**	**4678.31**	**4677.31**	**4677.16**	**4,677.2**	**4,677.0**	**4677.267**	**4,677.17**	**4677.06**
Mean (Ib)	N/A	N/A	4681.61	4680.08	4680.12	4679.06	4678.62	4,678.1	4,677.2	4677.909	4,677.88	4677.97
Stdev (Ib)	N/A	N/A	2.51	1.89	1.016	2.07	0.95	0.9	0.1	0.455	0.72	0.33
CV (−)	**0.0031**	**None**	**None**	**None**	**None**	**None**	**None**	**None**	**None**	**None**	**None**	**None**
NSA	**125,000**	**500,000**	**11,402**	**7,267**	**14,857**	**19,890**	**23,640**	**15,000**	**10,500**	**12,000**	**17,580**	**7,920**

Note: 1 in^{-2} = 6.452 cm^2; 1 lb. = 4.45 N.

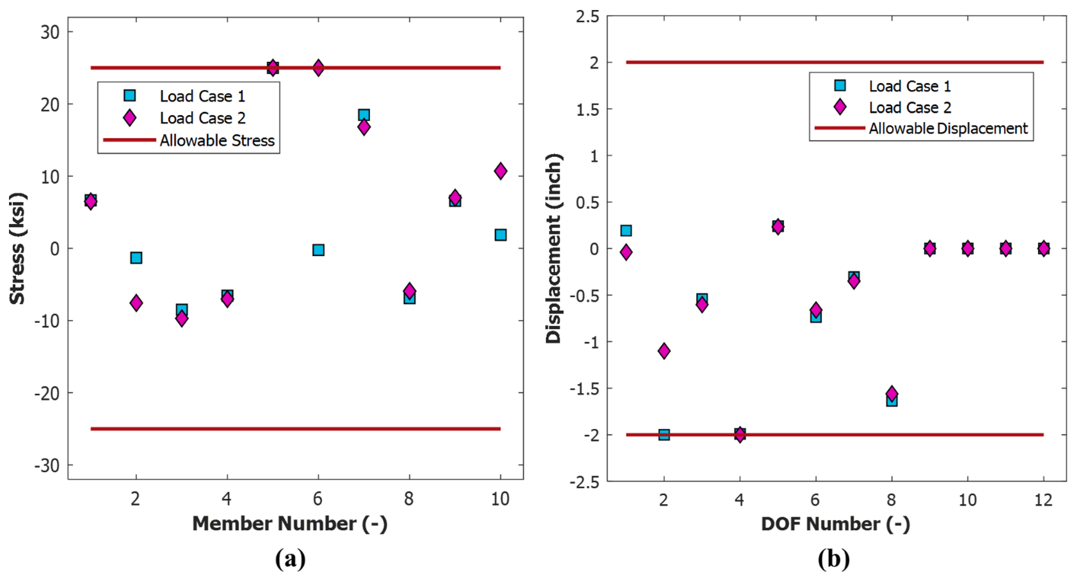

Fig. 4. Optimized result constraint values boundaries for the 10-bar truss structure (a) Stress constraint values (b) Displacement constraint values.

election campaign that takes into consideration societal needs and aspirations. Electoral district candidates from various parties may attempt to emulate previous constituency winners in their current campaigning efforts. This usually includes the adoption of some of the policies/slogans put forth by competing parties and follow advertising strategies that will help them gain the lead in elections. Moreover, party constituency candidates, although members of political parties themselves, play a dual-role and compete with other members of the same party for party leadership [32]. The changing of political alliance is another phenomenon that often occurs in parliamentary politics if party members believe that their chances of winning upcoming parliamentary elections are greater. The entire political process, therefore, whether it be electoral district election or party leadership, does not occur in a vacuum and has a central theme of competition and exclusion that occurs in many tiers. The simple fact is that parties and party members that perform well in general elections and are more organized in their campaigning effort win greater number of electoral districts and ultimately maximize their representation in parliament.

3.2. Operative sequence

The main focus of this study is to extend the application of the recently developed PO algorithm to the problem of weight minimization of truss structures. To effectively comprehend the phases of the algorithm, all relevant terms used to describe its operative sequence first require definition. The terms and their mathematical equivalent are listed below:

- **Party Member:** Candidate solution in d-dimensional search space
- **Party:** Logical grouping of party members
- **Constituency (Electoral District):** A hypothetical grouping of corresponding party members such that the first party member from every party are competing for the first constituency and the second members for the second constituency and so on.
- **Fitness:** Objective function value of a party member
- **Population:** Total number of party members in a solution space

The idea of the PO algorithm is based on mimicking all the major

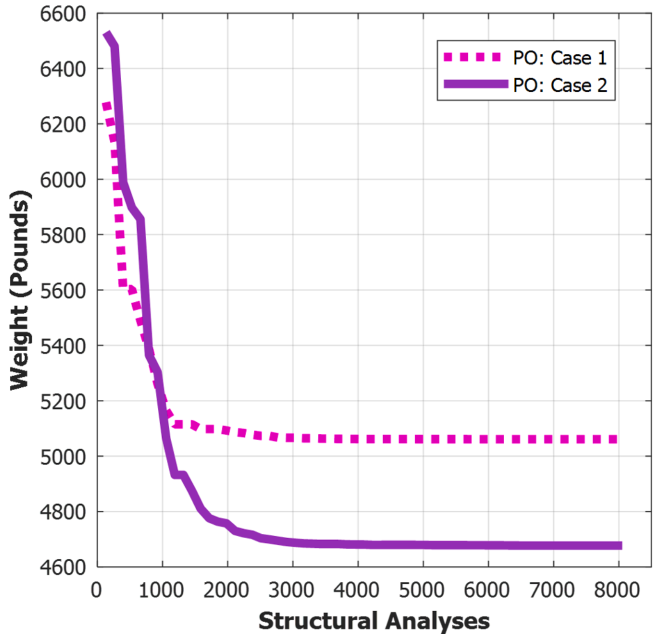

Fig. 5. Convergence plot for the 10-bar truss structure.

phases of parliamentary politics and the interactions that take place in them. In its entirety, the algorithm consists of five major steps: (1) Initialization, (2) Election Campaigning, (3) Party Switching, (4) General Elections, and (5) Parliamentary Affairs. Step (1) being performed only once, while steps 2 to 5 are carried out in a loop. A simple flowchart outlining the general algorithmic process is shown in Fig. 2. The algorithm begins by first dividing search agents into N number of political parties to serve as sub-populations that compete for local party leadership. Furthermore, party members are moreover divided among electoral districts (constituencies) in such a way that every corresponding party member from every party competes for the domination of a single constituency. In that regard, a dual population partitioning scheme along party and constituency lines are set up so as to maximize the explorative nature of the algorithm. Maintaining population diversity by dividing the population and hence search space into regions of interest is the main aim of these population-partitioning strategies. Fig. 1 shows a typical PO population division scheme where it is evident that the number of active parties and sought after constituencies are equally divided. Population size, therefore, is governed by the number of political parties and constituencies and is simply the product of the two variables ($PopSize = N_{parties} \times N_{constituency}$). Every party is headed by its fittest member, also known as a "party leader," and party members update their positions iteratively first according to local party leaders and then local constituency winners. This position updating strategy ensures that the population of search agents collectively move toward optimal solutions without the danger of premature convergence. Global exploration is achieved by a random operator that iteratively decreases over time which swaps party members with each other. This shuffling effect facilitates the transfer of information amongst every party independently and helps to avoid unwanted premature convergence. To further enhance comprehension, a brief mathematical description of all the major steps in the PO algorithm is presented as follows:

3.2.1. *Initialization*

Like other metaheuristic algorithms, PO starts by randomly generating the initial population of agents in d-dimensional search space between the upper and lower design variable bound as:

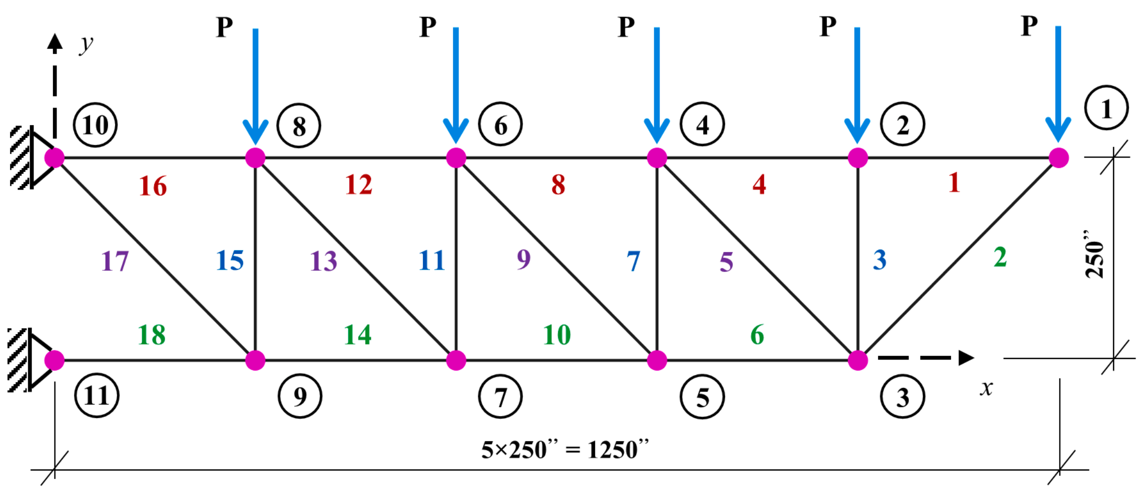

Fig. 6. Schematic of the 18-bar planar truss structure.

Table 5
Optimized results for the 18-bar planar truss.

Design variable (in^2)	Imai & Schmit [41] (Multiplier Method)	Lee & Geem [10] (HS)	Sonmez [8] (ABC-AP)	Khatibinia & Yazdani [30] (MGSA)	(AMGSA)	This study (PO)
A_1	9.998	9.980	10.000	10.000	10.000	10.000
A_2	21.65	21.63	21.651	21.651	21.651	21.651
A_3	12.50	12.49	12.500	12.500	12.500	12.500
A_4	7.072	7.057	7.071	7.071	7.071	7.071
Weight **(Ib)**	**6430.0**	**6421.88**	**6430.529**	**6430.529**	**6430.529**	**6430.529**
Mean **(Ib)**	N/A	N/A	N/A	6431.0	6430.529	6430.529
Stdev **(Ib)**	N/A	N/A	N/A	0.0	0.0	0.0
CV (–)	**0.258×10^{-3}**	**7.58×10^{-3}**	**None**	**None**	**None**	**None**
NSA	**N/A**	**2,000**	**200,000**	**15,000**	**10,500**	**3,564**

Note: 1 in^{-2} = 6.452 cm^2; 1 lb. = 4.45 N.

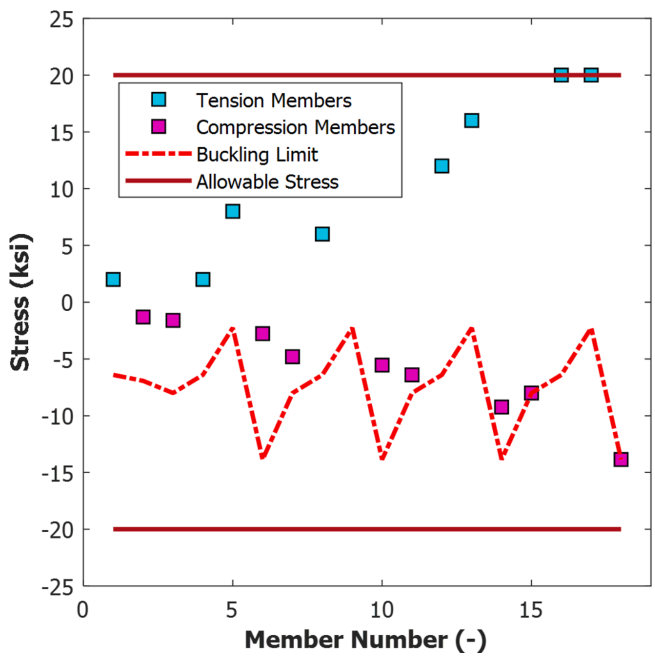

Fig. 7. Optimized result stress constraint values for the 18-bar truss structure.

$$x_{i,j} = x_L + r \times (x_U - x_L) \qquad i = 1, 2, 3, \cdots, PopSize \tag{11}$$

where x_U and x_L are the upper and lower design variable bounds of the *jth* coordinate for the *ith* design variable, respectively, and r is a random number generated in the range of [0,1] that follows a Gaussian distribution.

It's important to note here that the party formation and constituency allocation steps are both included in the initialization phase. Party members X are first equally divided among N number of political parties P such that the number of members in each party is equivalent to the number of parties in the search space. This is mathematically expressed as:

Table 7
Structural member stress limitations (ksi) for the 22-bar truss.

Design Variable	Member Grouping	Tensile Limit	Compressive Limit
1	$A_1 \sim A_4$	36.0	24.0
2	$A_5 \sim A_6$	36.0	30.0
3	$A_7 \sim A_8$	36.0	28.0
4	$A_9 \sim A_{10}$	36.0	26.0
5	$A_{11} \sim A_{14}$	36.0	22.0
6	$A_{15} \sim A_{18}$	36.0	20.0
7	$A_{19} \sim A_{22}$	36.0	18.0

Note: 1 ksi = 6.897 MPa.

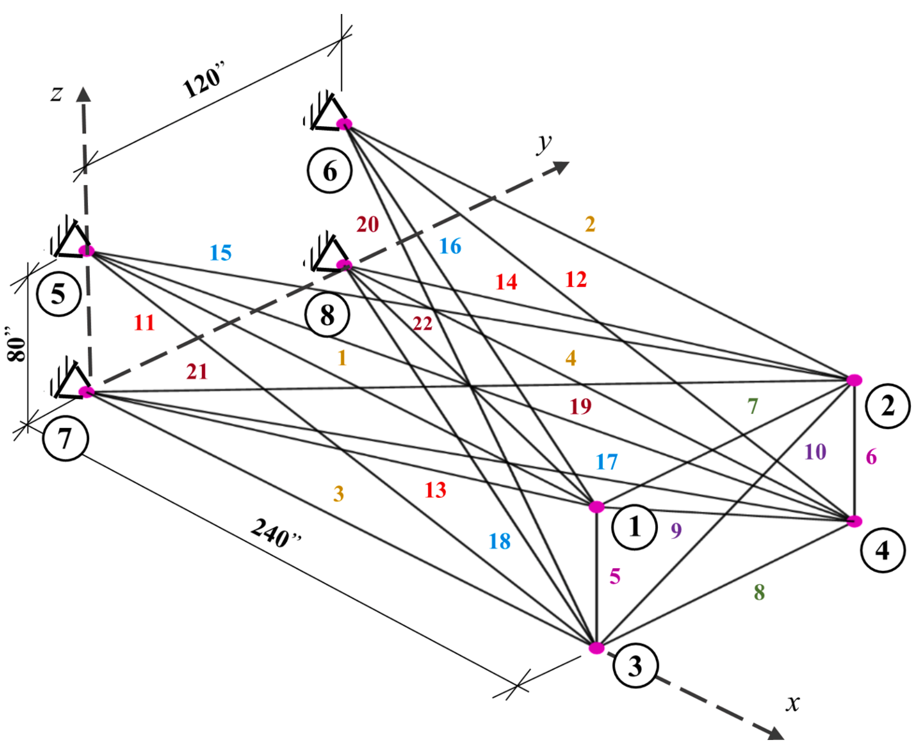

Fig. 8. Schematic of the 22-bar spatial truss structure.

Table 6
Loading condition (kips) for the 22-bar truss structure.

Node	Case 1			Case 2			Case 3		
	x	y	z	x	y	z	x	y	z
1	−20.0	0.0	−5.0	−20.0	−5.0	0.0	−20.0	0.0	35.0
2	−20.0	0.0	−5.0	−20.0	−50.0	0.0	−20.0	0.0	0.0
3	−20.0	0.0	−30.0	−20.0	−5.0	0.0	−20.0	0.0	0.0
4	−20.0	0.0	−30.0	−20.0	−50.0	0.0	−20.0	0.0	−35.0

Note: 1 kips = 4.45 kN.

Table 8
Optimized results for the 22-bar spatial truss.

Design variable (in^2)	Sheu & Schmit [42]	Khan & Willmert [43]	Lee & Geem [10] (HS)	Li et al. [6] (HPSO)	Talatahari et al. [44]		Kaveh et al. [28] (HPSSO)	Kaveh & Bakhshpoori [20] (WEO)	Jalili & Kashan [45]		This study (PO)
					(PSO)	(MSPSO)			(EM-MS)	(OIO)	
A_1	2.629	2.563	2.588	3.157	2.5799	2.6320	2.620593	2.6196	2.64791	2.651604	2.6211
A_2	1.162	1.553	1.083	1.269	1.1312	1.1952	1.206836	1.1344	1.17990	1.210872	1.1632
A_3	0.343	0.281	0.363	0.980	0.3472	0.3541	0.355719	0.3461	0.35681	0.347109	0.34855
A_4	0.423	0.512	0.422	0.100	0.4212	0.4145	0.419223	0.4218	0.42000	0.416448	0.41798
A_5	2.782	2.626	2.827	3.280	2.8330	2.7644	2.783028	2.8002	2.76075	2.745817	2.7864
A_6	2.173	2.131	2.055	1.402	2.0946	2.0297	2.082686	2.1261	2.07069	2.061166	2.0831
A_7	1.952	2.213	2.044	1.301	2.0205	2.0909	2.029553	1.9849	2.04131	2.059095	2.0331
Weight (Ib)	**1,024.80**	**1034.74**	**1022.23**	**977.81**	**1024**	**1024**	**1023.9857**	**1023.9703**	**1023.99**	**1023.9730**	**1023.89**
Mean (Ib)	N/A	N/A	N/A	N/A	1033.8	1028.6	1027.599	1024.5075	1025.76	1025.039	1024.12
Stdev (Ib)	N/A	N/A	N/A	N/A	17.69	6.63	6.357	0.73	2.16	0.80	0.71
CV (−)	**None**	**None**	**0.0080**	**4.217**	**None**	**None**	**None**	**None**	**None**	**None**	**None**
NSA	**N/A**	**N/A**	**10,000**	**N/A**	**25,000**	**12,500**	**14,406**	**19,510**	**17,000**	**15,300**	**8,976**

Note: 1 in^{-2} = 6.452 cm^2; 1 lb. = 4.45 N.

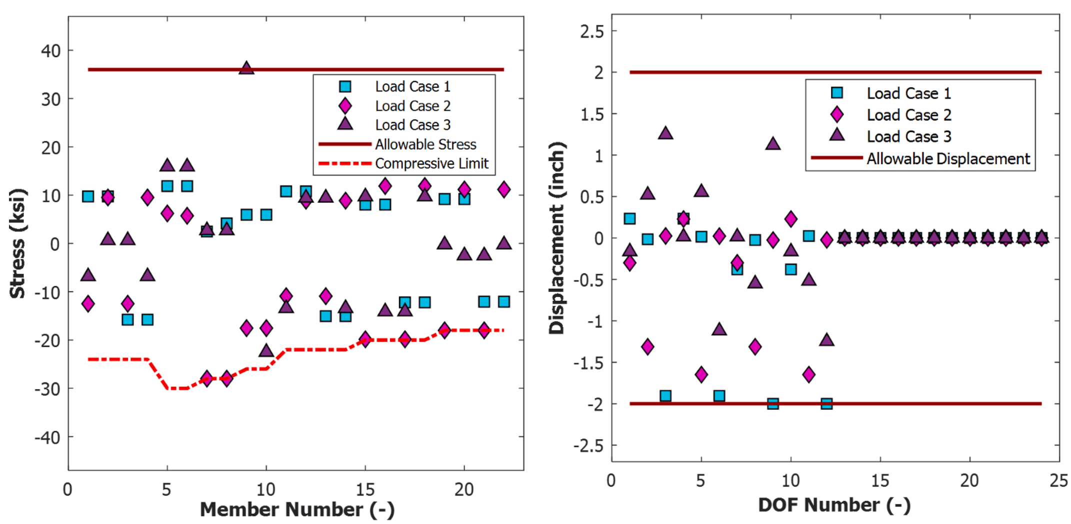

(a) **(b)**

Fig. 9. Optimized result constraint values for the 22-bar truss structure (a) Stress constraint values (b) Displacement constraint values.

$$P_i = \{X_1, X_2, X_3, \cdots, X_N\} \qquad i = 1, 2, 3 \cdots N \tag{12}$$

$$\wp = \{P_1, P_2, P_3, \cdots, P_N\} \tag{13}$$

where $\wp$ represents the set of all parties in the search space.

Based off these new found party formations, a set of N constituencies C, equivalent in number to the number of parties ($N = N_{parties} = N_{constituency}$), comprised of every corresponding party member in every party, are grouped together. Every *cth* constituency member competes with every other corresponding member for constituency leadership. The grouping of party members in every corresponding constituency is hence written as:

$$C_c = \{X_1^c, X_2^c, X_3^c, \cdots, X_N^c\} \qquad c = 1, 2, 3 \cdots N \tag{14}$$

Following party formation and constituency allocation comes the evaluation of party member fitness. Also known as the election phase, the objective function value of every search agent is evaluated with respect to its position vector. Party leaders X^* (*best individual from every party*) and constituency winners C^* (*best fitness value among every cth constituency*) are grouped together as shown in Eq. 15 and Eq. 16, respectively:

$$P^* = \{X_1^*, X_2^*, X_3^*, \cdots, X_N^*\} \tag{15}$$

$$C^* = \{C_1^*, C_2^*, C_3^*, \cdots, C_N^*\} \tag{16}$$

3.2.2. Election campaign (Exploitation)

Party members update their position values in this step. The adopted methodology makes use of a solution agent's current and previous fitness value in order to mathematically estimate a new position that would improve their fitness. This novel position updating technique is known as the recent past-based position updating strategy (RPPUS) [32]. Furthermore, to incorporate swarm-like behavior, every party member is first updated with respect to their local party leaders and then local constituency winners. Represented as m^* in Eq. 17 and 18. This ensures that party members in every party thoroughly investigate its region of the search space without the dangers of premature convergence.

Mathematically, candidate solutions update their position values based on two scenarios: (1) if a party member's current fitness value $f(X_i(t))$ is better than its previous one $f(X_i(t-1))$, then Eq. 17 is used (2) if, on the other hand, fitness values are found to be worse than the previous value, Eq. 18 is adopted. This conditional step is carried out whether a candidate solution updates its position value according to its local party leader or constituency winner. Both of the previously mentioned equations loop through each *jth* coordinate of the *ith* party member competing for the *cth* constituency. In this way, every party member, in a sense, *learns* from its performance in previous elections and seeks better search zones.

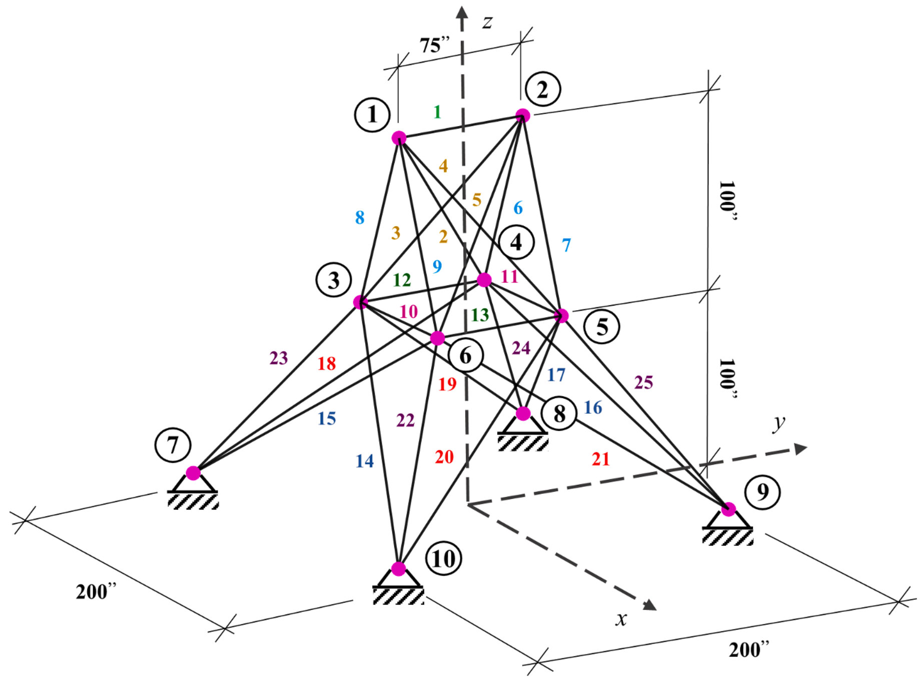

Fig. 10. Schematic of the 25-bar spatial truss structure.

It also indirectly moves away from worst solutions and towards better ones collectively. A more thorough explanation of the RPPUS position updating strategy can be found in reference [32].

$$x_{i,j}^c(t+1)=\begin{cases} m^*+r\left(m^*-x_{i,j}^c(t)\right) & \text{if } x_{i,j}^c(t-1)\le x_{i,j}^c(t)\le m^* \text{ or } x_{i,j}^c(t-1)\ge x_{i,j}^c(t)\ge m^* \\ m^*+(2r-1)\left|m^*-x_{i,j}^c(t)\right| & \text{if } x_{i,j}^c(t-1)\le m^*\le x_{i,j}^c(t) \text{ or } x_{i,j}^c(t-1)\ge m^*\ge x_{i,j}^c(t) \\ m^*+(2r-1)\left|m^*-x_{i,j}^c(t-1)\right| & \text{if } m^*\le x_{i,j}^c(t-1)\le x_{i,j}^c(t) \text{ or } m^*\ge x_{i,j}^c(t-1)\ge x_{i,j}^c(t) \end{cases} \tag{17}$$

$$x_{i,j}^c(t+1)=\begin{cases} m^*+(2r-1)\left|m^*-x_{i,j}^c(t)\right| & \text{if } x_{i,j}^c(t-1)\le x_{i,j}^c(t)\le m^* \text{ or } x_{i,j}^c(t-1)\ge x_{i,j}^c(t)\ge m^* \\ x_{i,j}^c(t-1)+r\left(x_{i,j}^c(t)-x_{i,j}^c(t-1)\right) & \text{if } x_{i,j}^c(t-1)\le m^*\le x_{i,j}^c(t) \text{ or } x_{i,j}^c(t-1)\ge m^*\ge x_{i,j}^c(t) \\ m^*+(2r-1)\left|m^*-x_{i,j}^c(t-1)\right| & \text{if } m^*\le x_{i,j}^c(t-1)\le x_{i,j}^c(t) \text{ or } m^*\ge x_{i,j}^c(t-1)\ge x_{i,j}^c(t) \end{cases} \tag{18}$$

Table 9
Structural member stress limitations (ksi) for the 25-bar truss.

Design Variable	Member Grouping	Tensile Limit	Compressive Limit
1	A_1	40.0	35.092
2	$A_2 \sim A_5$	40.0	11.590
3	$A_6 \sim A_9$	40.0	17.305
4	$A_{10} \sim A_{11}$	40.0	35.092
5	$A_{12} \sim A_{13}$	40.0	35.092
6	$A_{14} \sim A_{17}$	40.0	6.759
7	$A_{18} \sim A_{21}$	40.0	6.759
8	$A_{22} \sim A_{25}$	40.0	11.082

Note: 1 ksi = 6.897 MPa.

Table 10
Loading condition (kips) for the 25-bar truss structure.

Node	Case 1			Case 2		
	x	y	z	x	y	z
1	0.0	20.0	−5.0	1.0	10.0	−5.0
2	0.0	−20.0	−5.0	0.0	10.0	−5.0
3	0.0	0.0	0.0	0.0	0.0	0.0
6	0.0	0.0	0.0	0.0	0.0	0.0

Note: 1 kips = 4.45 kN.

Algorithm 1 Pseudo-code of the PO algorithm

Algorithm 1 Pseudo-code of the PO algorithm

Initialize the parameters *N*, λ, *and* t_{max} ;
Initialize the positions of party members X_i *(i = 1, 2, 3, …, PopSize);*
Divide population into political parties and constituencies and estimate initial fitness*;*
Initially set $f(X_i(t-1)) = f(X_i(t))$ for all candidate solutions;
While (t $\leq$ t$_{max}$) do
    Update value of adaptive parameter p according to **Eq.** (19);
    */*Election Campaign Phase*/* ***********************************
    For *every party member* $(i \rightarrow PopSize)$ **do**
        If $f(X_i(t)) \leq f(X_i(t-1))$ **do**
            For *every vector dimension* $(k \rightarrow d)$ **do**
                r = random number in the interval [0,1];
                m_p^* = *kth* local party leader position variable;
                m_c^* = *kth* local constituency winner position variable;
                Update X_i w.r.t m_p^* and then m_c^* using **Eq.** (17);
            End For
        Else If $f(X_i(t)) > f(X_i(t-1))$
            For *every vector dimension* $(k \rightarrow d)$ **do**
                r = random number in the interval [0,1];
                m_p^* = *kth* local party leader position variable;
                m_c^* = *kth* local constituency winner position variable;
                Update X_i w.r.t m_p^* and then m_c^* using **Eq.** (18);
            End For
        End If
    End For
    */*Party Switching Phase*/* ***********************************
    For *every party* $(i \rightarrow N_{parties})$ **do**
        For *each party member of ith party* $(j \rightarrow n)$ X_j **do**
            r = random number in the interval [0,1]
            If $r < p$ **do**
                rP = random integer (party) in the interval [0, $N_{parties}$];
                Determine least fit member in selected party (X_{worst})
                swap (X_{worst}, X_j)
            End If
        End For
    End For
    */*General Election Phase*/* ***********************************
    Calculate new fitness values and update party leaders and constituency winner listing;
    Update party and constituency boundaries based on **Eq.** (12) and (14);
    */*Parliamentary Affairs Phase*/* ***********************************
    For *each constituency* $(i \rightarrow N_{constituency})$ **do**
        rC = random integer (constituency) in the interval [0, $N_{constituecny}$]
        C_{rC}^* = position vector of constituency winner in electoral district rC;
        Update position of C_i^* w.r.t C_{rC}^* using **Eq.** (20);
        Replace position and fitness values of C_i^* with C_{new}^* only if fitness value improves
    End For
    $t = t + 1$;
End While
Return *bestFitness, X_b;*

Table 11
Optimized results for the 25-bar spatial truss.

Design variable (in^2)	Camp & Bichon [7] (ACO)	Li *et al.* [6] (PSO)	(PSOPC)	(HPSO)	Sonmez [8] (ABC-AP)	Kaveh & Zakian [29] (BA)	Kaveh *et al.* [28] (HPSSO)	Camp & Farshchin [27] (mTLBO)	Kaveh & Bakhshpoori [20] (WEO)	Kaveh & Zolghadr [39] (CPA)	Kaveh *et al.* [40] (PGO)	This study (PO)
A_1	0.0100	9.863	0.010	0.010	0.0110	0.0100	0.01	0.0100	0.01	0.0100	0.0100	0.010038
A_2	2.0000	1.798	1.979	1.970	1.9790	1.97889	1.9907	1.9878	1.9814	1.9890	1.9908	1.9797
A_3	2.9660	3.654	3.011	3.016	3.0030	3.00472	2.9881	2.9914	3.0023	2.9880	2.9872	3.0052
A_4	0.0100	0.100	0.100	0.010	0.0100	0.01000	0.0100	0.0102	0.0100	0.0100	0.0100	0.01
A_5	0.0120	0.100	0.100	0.010	0.0100	0.01000	0.0100	0.0100	0.0100	0.0100	0.0100	0.010018
A_6	0.6890	0.596	0.657	0.694	0.6900	0.68880	0.6824	0.6828	0.6827	0.6980	0.6824	0.68165
A_7	1.6790	1.659	1.678	1.681	1.6790	1.67834	1.6764	1.6775	1.6778	1.6780	1.6769	1.6779
A_8	2.6680	2.612	2.693	2.643	2.6520	2.65270	2.6656	2.6640	2.6612	2.6580	2.6658	2.6617
Weight (Ib)	**545.530**	**627.08**	**545.27**	**545.19**	**545.19**	**545.168**	**545.164**	**545.175**	**545.166**	**545.18**	**545.172**	**545.165**
Mean (Ib)	546.340	N/A	N/A	N/A	N/A	546.446	545.556	545.483	545.226	545.49	545.392	545.45
Stdev (Ib)	0.94	N/A	N/A	N/A	N/A	N/A	0.432	0.306	0.083	0.24	0.391	0.21
CV (−)	**None**	**None**	**None**	**None**	**None**	**None**	**None**	**None**	**None**	**None**	**None**	**None**
NSA	**16,500**	**150,000**	**150,000**	**125,000**	**500,000**	**20,000**	**13,326**	**12,199**	**19,750**	**22,800**	**17,880**	**8,316**

Note: 1 in^{-2} = 6.452 cm^2; 1 lb. = 4.45 N.

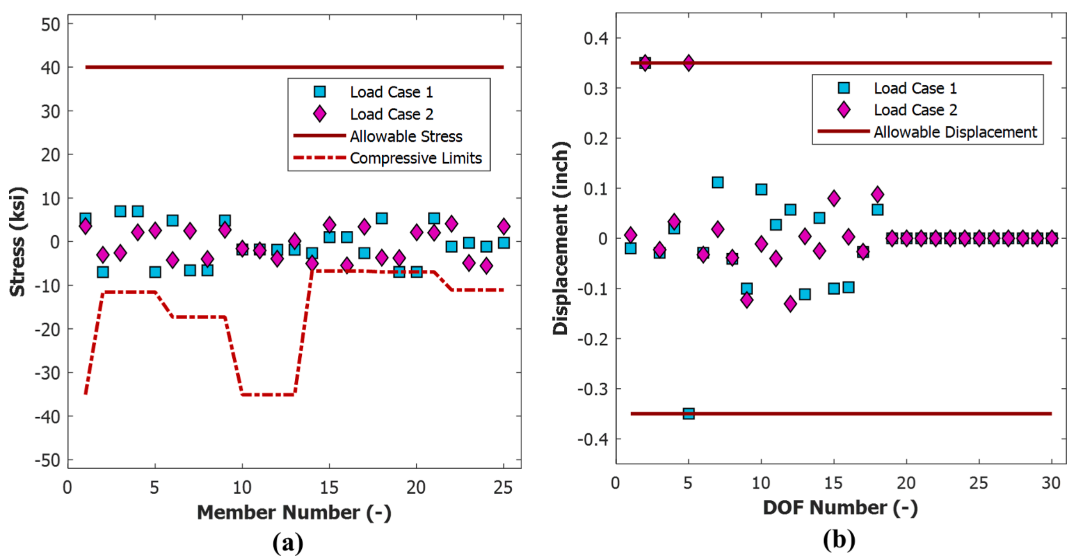

Fig. 11. Optimized result constraint values for the 25-bar truss structure (a) Stress constraint values (b) Displacement constraint values.

3.2.3. *Party switching (Balancing exploitation with Exploration)*

Metaheuristics often become trapped in local optima whenever they are close to the optimum solutions. In order to tackle this issue, all party members X_i are allowed to switch parties with the least fittest members of another randomly chosen party. The probability of a party member being selected for swapping is governed by an adaptive parameter p whose value decreases iteratively from 1 to 0 according to Eq. 19

$$p = \lambda \times \left(\frac{t_{max} - t}{t_{max}}\right) \tag{19}$$

where λ is the party switching rate parameter, t_{max} is the maximum number of iterations, and t is the current iteration value. Since this is an iterative dependent process, this phase serves as an exploration–exploitation controller. By adjusting the party switching parameter value λ, an efficient balance between these two search aspects for any given problem is achieved.

3.2.4. *General elections (Fitness Determination)*

In this phase, the fitness values of all updated solution vectors are evaluated. New party leaders and constituency winners based on the changes carried in the previous steps are determined and grouped together according Eq. 15 and 16. The updating of political party and constituency groupings throughout the optimization process, given any changes, is sometimes conveniently referred to as "Government Formation." This implies that new party and constituency boundaries are formed according to the election results.

3.2.5. *Parliamentary Affairs (Exploitation and Convergence)*

Finally, as an added exploitation phase, every parliamentarian C_i^* (constituency winners) update their position vectors with reference to a randomly chosen constituency winner C_r^* from another contested constituency according to Eq. 20. New fitness values are subsequently calculated and the updated position is recorded only if an improvement of fitness value is observed whereas no position values are changed if objective function values worsen. In that regard, a fly-back mechanism is incorporated in this final phase and incremental improvement among constituency members is achieved iteratively independent of party leaders.

$$C_i^* = C_r^* + (2r - 1)|C_r^* - C_i^*| \tag{20}$$

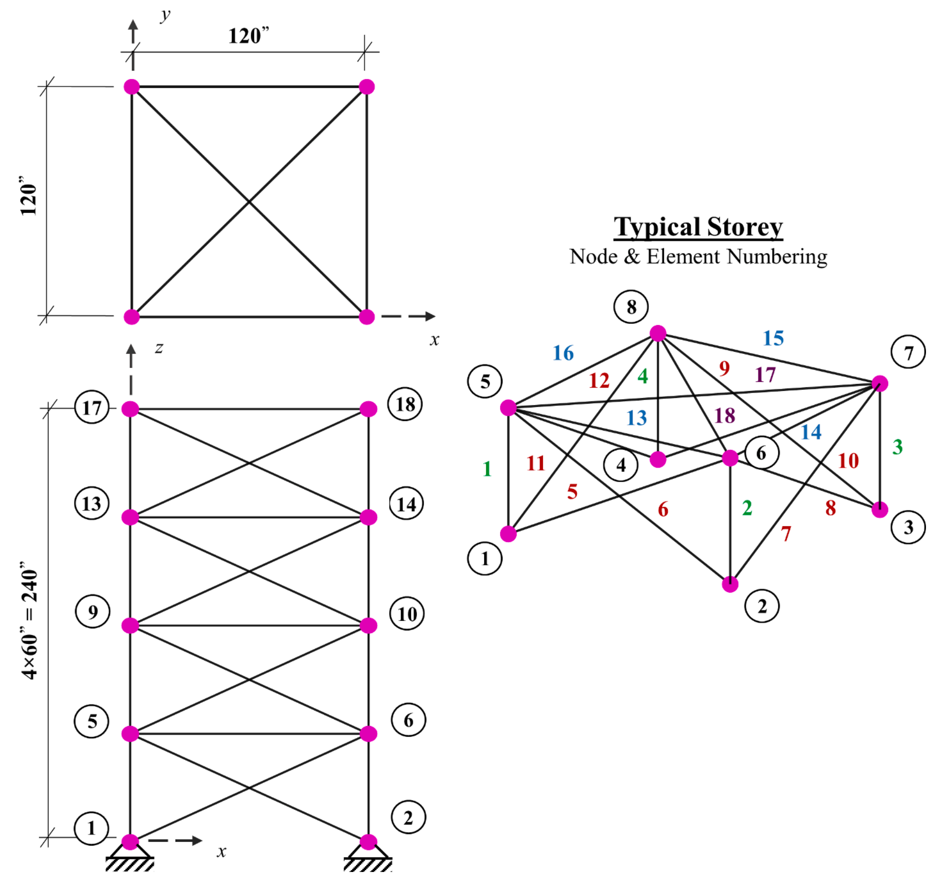

Fig. 12. Schematic of the 72-bar spatial truss structure.

Table 12
Loading conditions (kips) for the 72-bar truss structure.

Node	Condition 1			Condition 2		
	x	y	z	x	y	z
17	5.0	5.0	−5.0	0.0	0.0	−5.0
18	0.0	0.0	0.0	0.0	0.0	−5.0
19	0.0	0.0	0.0	0.0	0.0	−5.0
20	0.0	0.0	0.0	0.0	0.0	−5.0

Note: 1 kips = 4.45 kN.

Table 13
Element grouping for the 72-bar planar truss.

Design Variable	Member Grouping	Design Variable	Member Grouping
A_1	1, 2, 3, 4	A_9	37, 38, 39, 40
A_2	5, 6, 7, 8, 9, 10, 11, 12	A_{10}	41, 42, 43, 44, 45, 46, 47, 48
A_3	13, 14, 15, 16	A_{11}	49, 50, 51, 52
A_4	17, 18	A_{12}	53, 54
A_5	19, 20, 21, 22	A_{13}	55, 56, 57, 58
A_6	23, 24, 25, 26, 27	A_{14}	59, 60, 61, 62, 63, 64, 65, 66
A_7	31, 32, 33, 34	A_{15}	67, 68, 69, 70
A_8	35, 36	A_{16}	71, 72

The PO algorithm can therefore be superimposed to the problem of truss optimization in the following way: party members represent candidate truss designs solutions, election outcomes in the form of fitness values correspond to the penalized weight of any structural system, and party leaders and constituency winners represent feasible light weight designs for a given sub-collection of optimized trusses.

4. Numerical examples

A total of seven truss structural systems with multiple loading conditions and design constraints were chosen as benchmarks to demonstrate the effectiveness of the PO algorithm. Based on their sizes, the problems can be divided into two groups. The first group includes the small/medium scale trusses which are represented by the 10 bar, 18 bar, 22 bar, 25 bar, and 72 bar structural systems, while the second group comprises of the larger trusses given as the 200 bar and 942 bar spatial truss tower. The larger structural systems were chosen to demonstrate the feasibility of the PO algorithm at optimizing real-sized structures. For all problems, the *direct stiffness* method of analysis was adopted and optimized results were validated by comparison with those published previously in literature. As per the recommendations and guidelines laid down by Ref. [32], the effects of only two tuning parameters on algorithmic performance were investigated in this study, i.e., N (number of parties/constituencies) and λ (party switching rate). After a thorough sensitivity analysis, in which the influence of each parameter was studied independently, it was found that a value of 11 for N and 0.5 for λ was most effective in balancing between exploration and exploitation. Finally, to account for the algorithm's stochastic nature, the best and mean weight as well as the standard deviation of 50 independent runs were tabulated for every problem. The PO algorithm was coded in the MATLAB programming environment and executed on a laptop having a 1.6 GHz Intel Duo Core processor with 4 GB of memory.

4.1. Planar 10-bar truss structure

A standard problem often found in literature, the 10 bar planar truss structure has long served as a sizing benchmark by many researchers

Table 14
Optimized results for the 72-bar spatial truss (Case 1).

Design variable (in^2)	Lee & Geem [10] (HS)	Li *et al.* [6] (PSO)	Li *et al.* [6] (PSOPC)	Li *et al.* [6] (HPSO)	Sonmez [8] (ABC-AP)	Degertekin [37] (EHS)	Degertekin [37] (SAHS)	Degertekin [15] (TLBO)	Kaveh *et al.* [20] (WEO)	Javidi *et al.* [31] (CSA)	Javidi *et al.* [31] (ECSA)	Kooshkbaghi & Kaveh [21] (ACCS)	This study (PO)
A_1	1.963	40.053	1.652	1.907	1.8907	1.889	1.889	1.8929	1.8616	1.9222	1.8899	1.836	1.8812
A_2	0.481	0.237	0.547	0.524	0.5166	0.502	0.520	0.5160	0.5206	0.5897	0.5181	0.5059	0.52207
A_3	0.010	21.692	0.100	0.010	0.0100	0.010	0.010	0.0100	0.0105	0.0599	0.0101	0.0108	0.01003
A_4	0.011	0.657	0.101	0.010	0.0100	0.010	0.010	0.0100	0.0100	0.2848	0.0100	0.0103	0.010024
A_5	1.233	22.144	1.102	1.288	1.2968	1.284	1.289	1.2917	1.2455	2.3919	1.2548	1.2836	1.3045
A_6	0.506	0.266	0.589	0.523	0.5191	0.526	0.524	0.5176	0.5177	0.4194	0.5133	0.5388	0.51551
A_7	0.011	1.654	0.011	0.010	0.0100	0.010	0.010	0.0100	0.0101	0.1121	0.0100	0.0106	0.010011
A_8	0.012	10.284	0.010	0.010	0.0101	0.010	0.010	0.0100	0.0100	0.0473	0.0100	0.0108	0.010067
A_9	0.538	0.559	0.581	0.544	0.5208	0.528	0.539	0.5229	0.5327	0.8734	0.5431	0.5328	0.52429
A_{10}	0.533	12.883	0.458	0.528	0.5178	0.525	0.519	0.5193	0.5109	0.4344	0.5180	0.5184	0.51519
A_{11}	0.010	0.138	0.010	0.019	0.0100	0.010	0.015	0.0100	0.0100	0.0144	0.0100	0.0113	0.011122
A_{12}	0.167	0.188	0.152	0.020	0.1048	0.063	0.105	0.0997	0.1205	0.1297	0.1175	0.124	0.10444
A_{13}	0.161	29.048	0.161	0.176	0.1675	0.173	0.167	0.1680	0.1655	0.1631	0.1656	0.1651	0.16738
A_{14}	0.542	0.632	0.555	0.535	0.5346	0.550	0.532	0.5359	0.5397	0.4707	0.5438	0.5402	0.53737
A_{15}	0.478	3.045	0.514	0.426	0.4443	0.444	0.425	0.4457	0.4554	0.8557	0.4398	0.433	0.44244
A_{16}	0.551	1.711	0.648	0.612	0.5803	0.592	0.579	0.5818	0.5995	0.4239	0.5752	0.5745	0.57549
Weight (Ib)	**364.33**	**5417.02**	**368.45**	**364.86**	**363.8683**	**364.36**	**364.05**	**363.841**	**363.9827**	**413.96**	**363.89**	**364.147**	**363.88**
Mean (Ib)	N/A	N/A	N/A	N/A	N/A	366.79	366.57	364.42	364.3536	509.76	366.02	364.335	364.315
Stdev (Ib)	N/A	N/A	N/A	N/A	N/A	2.05	2.02	0.49	0.2188	41.29	2.12	0.186	0.181
CV (−)	**0.0039**	**None**	**None**	**None**	**None**	**None**	**None**	**None**	**None**	**None**	**None**	**None**	**None**
NSA	**20,000**	**150,000**	**125,000**	**125,000**	**400,000**	**13,755**	**12,852**	**17,954**	**19,860**	**22,342**	**16,892**	**12,000**	**8,448**

Note: 1 in^{-2} = 6.452 cm^2; 1 lb. = 4.45 N.

using either continuous or discrete sizing variables. Fig. 3 shows the layout and loadings for the truss under investigation. In this study, two loading cases were investigated: Case I involves load values of $P_1 = 100$ kips and $P_2 = 0$, while Case II optimizes the structure with $P_1 = 150$ kips and $P_2 = 50$ kips. It was assumed that all structural members are made from a material having a mass density of 0.10 lb./in^3 and elastic modulus of 10,000 ksi. Each member was regarded as an independent design variable whose value was to be selected from a maximum and minimum value range from $A_{min} = 0.1$ in^2 and $A_{max} = 35.0$ in^2. Allowable member stresses and nodal displacement limits were set as $\pm 25ksi$ and $\pm 2in$ for all free nodes in the x and y direction, respectively. In its entirety, the problem has a total of 32 non-linear design constraints (10 tension, 10 compression, and 12 displacement constraints).

4.1.1. PO parameter sensitivity analysis

The parameter sensitivity analysis for the PO algorithm is presented in this section. As mentioned earlier, one of the prime advantages of the PO algorithm over those presented literature is its relatively few performance parameters that influence solution quality. The effects of two parameters are investigated in this work, namely N (number of political parties/constituencies) and λ (party switching rate). The 10-bar planar truss structure has been selected as a benchmark problem for this purpose, and after a considerable amount of trial and error, an upper limit of 8,500 functional analyses was imposed. The parameters were tuned by adopting the "One-parameter-at-a-time" approach. Base nominal values for both N and λ are first chosen, and then one of the parameter is changed incrementally while the other remains fixed. This process continues for all variables and it allows to quantitatively determine both the general trend as well as the effects each have on the algorithm independently.

Nominal values of 8 and 0.5 were set for both N and λ, respectively, and as is clearly evident from Table 1, the effects of increasing the number of political parties (N), studied in the range from 2 to 15, decreases the best, worst, mean, and standard deviation of 50 independent runs. This behavior is consistent even when taking into account the stochastic nature of the algorithm. The trend holds true until the number of political parties reaches 11, where the algorithm obtains the best optimized structural weight with the lowest standard deviation, and begins to steadily increase beyond that.

In contrast, when the effects of the party switching rate parameter is investigated, sensitivity results tend to indicate a sense of stochastic behavior. The value of λ was varied in the range of 0.1 to 1.1 with N kept at its nominal value of 8. It can be inferred from the findings that the effect of λ on structural optimization performance is not that profound in comparison to the number of political parties. Nevertheless, considering the tabulated results of the standard deviation in Table 2, a general trend can be seen of an overall reduction in optimized weight discrepancy (standard deviation) and a greater algorithmic stability. Best overall optimization performance was achieved at a party switching rate value of 0.5 where the algorithm achieved best mean weight, worst weight and standard deviation among all runs

Based off these results, a combination of 11 and 0.5 for the number of political parties and party switching rate was found to be optimal. This implies an algorithmic population size of 121 party members The best optimized weight obtained from these findings was 5060.85 Ib. with a standard deviation of 0.53 for the first loading case of the 10-bar structure. For the remainder of this study, unless stated otherwise, a value of 11 for N and 0.5 for λ has been selected as performance parameters.

4.1.2. Result comparison with other optimizers in literature

A comparison of the results obtained for both loading scenarios of the 10-bar benchmark by the PO algorithm and other optimization methods in literature is presented in Tables 3 and 4. Combined convergence plots (i.e. structural weight vs. number of structural analyses) for each loading case is illustrated in Fig. 5. A final weight of 5060.85 Ib and 4677.06 Ib was achieved in 7,920 structural analyses for each of the cases with the proposed method. As evident from Fig. 4, none of the member stresses or nodal displacement values violate the predefined design constraints. A quick glance at tabulated results clearly demonstrate the inherent robustness and speed of the PO algorithm over many of the proposed optimization techniques present in literature. For Case I, the PO algorithm obtained the lightest structural design with the least amount of computational effort. Algorithms that achieved comparable results like

Table 15
Optimized results for the 72-bar spatial truss (Case 2).

Design variable (in^2)	Camp *et al.* [7] (ACO)	Camp [12] (BB-BC)	Kaveh & Khayatazad [47] (RO)	Kaveh & Zakian [29] (BA)	Kaveh & Ilchi Ghazaan [48]		Kaveh & Zakian [49] (IGWO)	Malihe *et al.* [46]			Kooshkbaghi & Kaveh [21] (ACCS)	Ozbasaran & Yildirim [50]		This study (PO)
					(CBO)	(ECBO)		(CA)	(EHO)	(EHOC)		(CSA)	(mCSA)	
A_1	1.948	1.8577	1.8365	1.85920	1.9170	1.8382	1.8585	1.7892	1.7012	1.8911	1.8665	1.5995	2.1050	1.8607
A_2	0.508	0.5059	0.5021	0.49308	0.5031	0.5259	0.5021	0.4571	0.4126	0.5051	0.5062	0.6009	0.5179	0.50626
A_3	0.101	0.1000	0.1000	0.10025	0.1000	0.1000	0.1002	0.1002	0.1000	0.1000	0.1	0.1005	0.1001	0.1
A_4	0.102	0.1000	0.1004	0.10178	0.1001	0.1000	0.1000	0.1000	0.1724	0.1000	0.1002	0.1105	0.1018	0.1
A_5	1.303	1.2476	1.2522	1.28534	1.2721	1.2622	1.3011	1.3200	1.1895	1.2778	1.2909	1.2956	1.1103	1.2749
A_6	0.511	0.5269	0.5033	0.51307	0.5050	0.5176	0.5151	0.5427	0.4376	0.5082	0.5177	0.4685	0.5214	0.50952
A_7	0.101	0.1000	0.1002	0.10073	0.1000	0.1000	0.1000	0.1000	0.1000	0.1004	0.1001	0.10001	0.1025	0.1
A_8	0.100	0.1012	0.1002	0.10248	0.1000	0.1000	0.1001	0.1000	0.1000	0.1000	0.1008	0.2368	0.1142	0.10012
A_9	0.561	0.5209	0.5730	0.51214	0.5184	0.5048	0.5311	0.5380	0.9084	0.5297	0.5148	0.3954	0.6183	0.52872
A_{10}	0.492	0.5172	0.5499	0.52547	0.5362	0.5174	0.5122	0.5377	0.4585	0.5343	0.5196	0.5015	0.5391	0.52359
A_{11}	0.1	0.1004	0.1004	0.10029	0.1000	0.1000	0.1008	0.1000	0.1000	0.1000	0.1001	0.1008	0.1010	0.10014
A_{12}	0.107	0.1005	0.1001	0.10297	0.1000	0.1004	0.1030	0.1000	0.1570	0.1000	0.1014	0.1035	0.1006	0.10001
A_{13}	0.156	0.1565	0.1576	0.15597	0.1569	0.1577	0.1560	0.1562	0.1356	0.1566	0.1567	0.1805	0.1568	0.15628
A_{14}	0.550	0.5507	0.5222	0.55473	0.5374	0.5437	0.5472	0.5593	1.1617	0.5431	0.5447	0.6675	0.5221	0.54998
A_{15}	0.390	0.3922	0.4356	0.40627	0.4062	0.4038	0.4202	0.4360	0.3279	0.4069	0.4176	0.36	0.4379	0.40132
A_{16}	0.592	0.5922	0.5972	0.59617	0.5741	0.5794	0.5793	0.5619	0.7093	0.5500	0.5601	0.7107	0.4491	0.58582
Weight (Ib)	**380.24**	**379.85**	**380.458**	**380.05819**	**379.75**	**379.84**	**379.7615**	**380.925**	**428.368**	**379.72**	**379.7512**	**394.7116**	**382.8231**	**379.68**
Mean (Ib)	383.16	382.08	382.5538	389.14389	380.03	380.18	380.6811	382.374	468.51	380.39	379.81	426.4132	402.3509	379.79
Stdev (Ib)	3.66	1.912	N/A	N/A	0.278	0.3544	0.7315	0.67	23.32	0.54	0.148	24.07941	17.95119	0.139
CV (–)	**None**	**None**	**None**	**None**	**None**	**None**	**None**	**None**	**None**	**None**	**None**	**None**	**None**	**None**
NSA	**18,500**	**19,621**	**19,084**	**20,000**	**18,000**	**18,000**	**11,960**	**19,650**	**9,680**	**8,400**	**12,000**	**150,000**	**150,000**	**7,788**

Note: 1 in^{-2} = 6.452 cm^2; 1 lb. = 4.45 N.

the Adaptive Penalty Artificial Bee Colony (ABC-AP) algorithm presented by Sonmez [8] was observed to be more computationally taxing. In particular, a total percentile reduction of 98.38% was recorded in comparison. On the other hand, algorithms such as the Efficient Harmony Search (EHS) and Self-Adaptive Harmony Search (SAHS) proposed by Degertekin [37] as well as the Magnetic Charge Search (MCSS) and the Improved Magnetic Charge Search (IMCSS) [38] were observed to have comparable computational efficiency but were found to have slightly heavier designs.

A similar inference has been made when the PO algorithm is applied to Case II of the benchmark. Among feasible results present in Table 4, the PO algorithm produced the lightest structural weight with the least number of structural analyses. The closest comparison in terms of final truss weight and convergence speeds that can be made with AMGSA [30] and SAHS, respectively. It should be noted that for SAHS, a heavier design was produced with about the same amount of computational effort. On the other hand, the opposite has been observed for AMGSA, where a 24.57% increase in computational effort over PO was recorded to reach comparable results.

In terms of algorithmic stability, the PO algorithm has demonstrated, for both loading scenarios, its superior performance by dint of its lower mean and standard deviation value in comparison with other proposed structural optimizers in literature. This was especially the case for scenario II of the benchmark. Barring the exceptions mentioned above, over all the PO algorithm, with its excellent explorative - exploitative mechanism, has allowed it have a near 100% success rate all the while ensuring that the feasible domain of the search space is thoroughly examined for the global optimum value.

4.2. Planar 18-bar truss structure

The second benchmark considered in this study is the 18-bar cantilever planar truss which is schematically depicted in Fig. 6. The structure was initially employed as a truss configuration problem but was later formulated as a structural sizing benchmark by Lee and Geem [10], Sonmez [8], and Khatibinia and Yazdani [30]. Comprising of 18 members and 11 nodes, the truss is subjected to a series of downward point loads of 20 kips acting on the upper free nodes. All members are assumed to be constructed from the same material with a mass density and elastic modulus of 0.10 lb./in^3 and 10,000 ksi, respectively. Allowable member stresses were limited to 20 ksi in both tension and compression. Furthermore, compressive members were subjected to buckling constraints in accordance with Euler's buckling limit which is calculated from,

$$\sigma_i^b = -\frac{KEA_i}{L_i^2} \tag{21}$$

where A_i and $L_i$are the cross-sectional area and length of the compressive load bearing members, respectively; E is the material's modulus of elasticity; and K is the effective length factor whose value depends on member cross-sectional geometry and is assumed to have a value of 4 [8]. Structural sizing variables were divided into four groups and are linked as follows: **(A_1)** 1, 4, 8, 12, and 16; **(A_2)** 2, 6, 10, 14, and 18; **(A_3)** 3, 7, 11, and 15; **(A_4)** 5, 9, 13, and 17. The lower and upper member cross-sectional area bounds are taken as A_{min} = 0.1 in^2 and A_{max} = 50.0 in^2. As a whole, the structural system has 36 non-linear design constraints (18 tension and 18 compression/buckling) and no nodal displacement limitations.

Table 5 compares the statistical findings of 50 indpendent runs for the PO algorithm with other metahueristic methods published in literature. Among optimized designs, the Harmony Search (HS) algorithm proposed by Lee and Geem [10] produced the lightest structure with a total weight of 6421.88 Ib. Upon further investigation, however, the result was found to violate pre-imposed design constraints by a factor of 7.5 × 10^{-3}. A similar finding was recorded for the design developed by

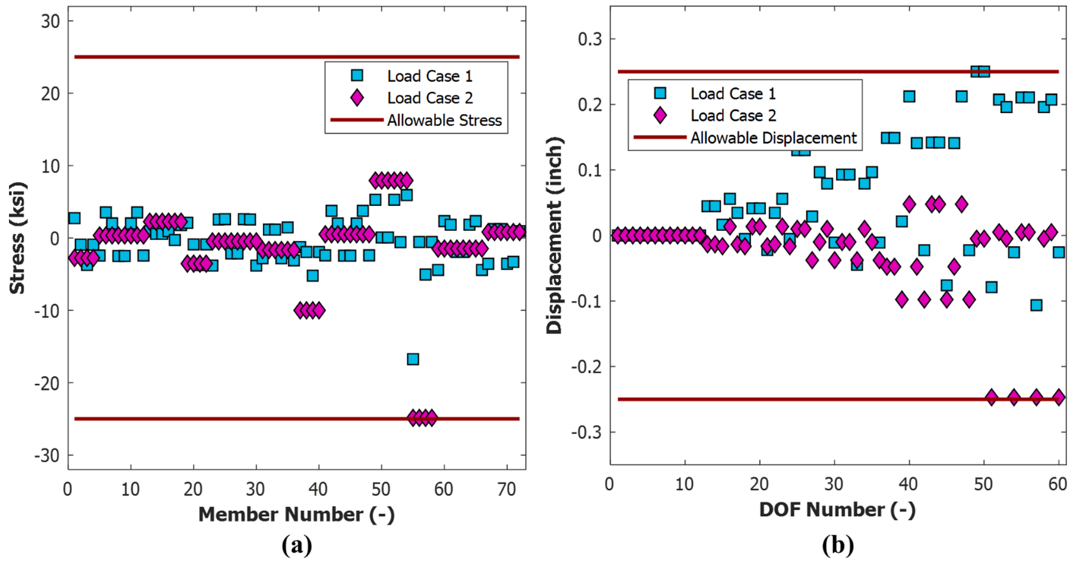

Fig. 13. Optimized result constraint values for the 72-bar truss structure (a) Stress constraint values (b) Displacement constraint values (Case 1).

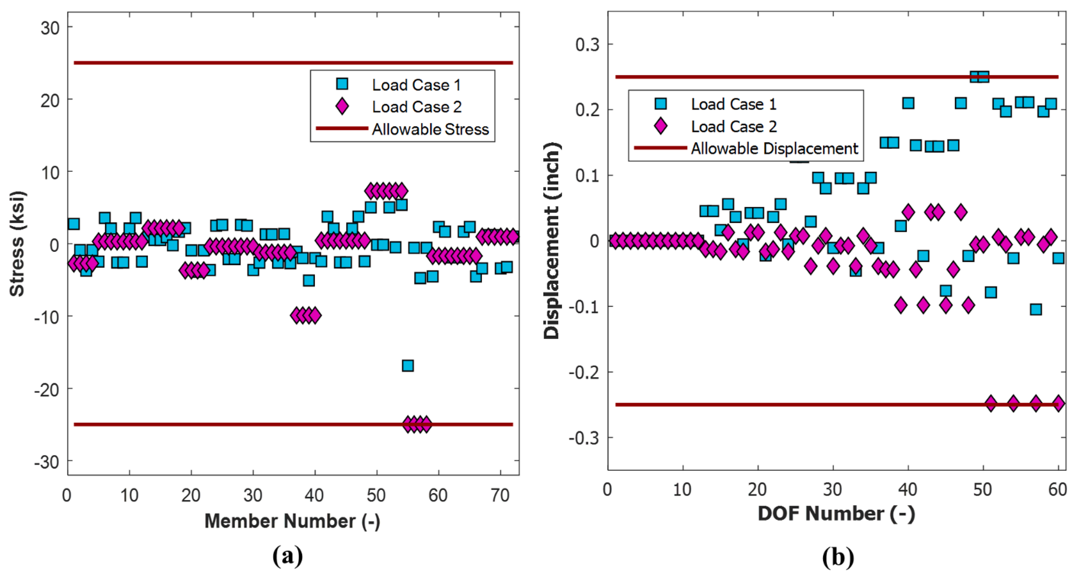

Fig. 14. Optimized result constraint values for the 72-bar truss structure (a) Stress constraint values (b) Displacement constraint values (Case 2).

Imai and Schmit [41] where a constraint violation of 0.258×10^{-3} was discovered. The ABC-AP [8], MGSA [30], AMGSA [30], and PO all produced similar final optimized weights of 6430.529 Ibs with no constraint violations. There is good reason to believe that this result represents the global optimum for the present benchmark under consideration. Fig. 7 depicts the stress values of both tension and compression members in relation to the imposed stress limitations for the final PO design. All values are shown to be within the range of the predefined design constraints. In addition, no compression members are reported to have a buckling stress value that exceeds the Euler limit.

In terms of convergence speeds, the PO algorithm outperformed the ABC-AP, MGSA, and AMGSA algorithms. An average CPU time of 4.5 s has been recorded per optimization cycle, and a total of 3564 structural analyses was required to reach convergence. That translates to a 66.05% reduction in computational effort compared to AMGSA, a 76.24% reduction compared to MGSA, and a 98.21% decrease from ABC-AP. Owing to the low dimensionality (number of design variables) of the 18-bar benchmark problem, no considerable variation in algorithmic stability is evident among feasibly produced designs. Most algorithms arrived at optimal solutions multiple times during the repeated computational runs. In that regard, the results obtained by the PO algorithm outperform all of those previously reported in literature.

4.3. Spatial 22-bar truss structure

Much like the previous benchmark, the 22-bar spatial truss, depicted in Fig. 8, was originally not intended to be a sizing problem. The structural system was first employed by Sheu and Schmit [42] as a topology optimization problem. It was later reformulated and adopted as a sizing benchmark by Lee and Geem [10], Li *et al.* [6], and Talatahari *et al.* [44]. Structural linkages are assumed to be constructed from a material having a mass density and elastic modulus of 0.10 lb./in^3 and 10,000 ksi, respectively. Member groupings and allowable tensile/compressive stress limits are shown in Table 7. The allowable displacements of all unsupported joints in every direction were limited to ± 2*in* and the maximum/minimum member cross-sectional areas for all members were set as $A_{min} = 0.1$ in^2 and $A_{max} = 4.0$ in^2. For this problem, three independent loading scenarios, described in Table 6, were

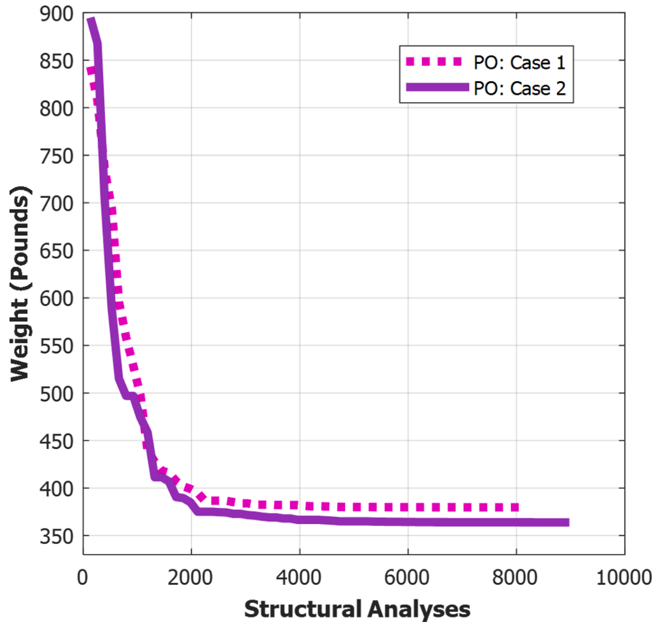

Fig. 15. Convergence plot for the 72-bar truss structure.

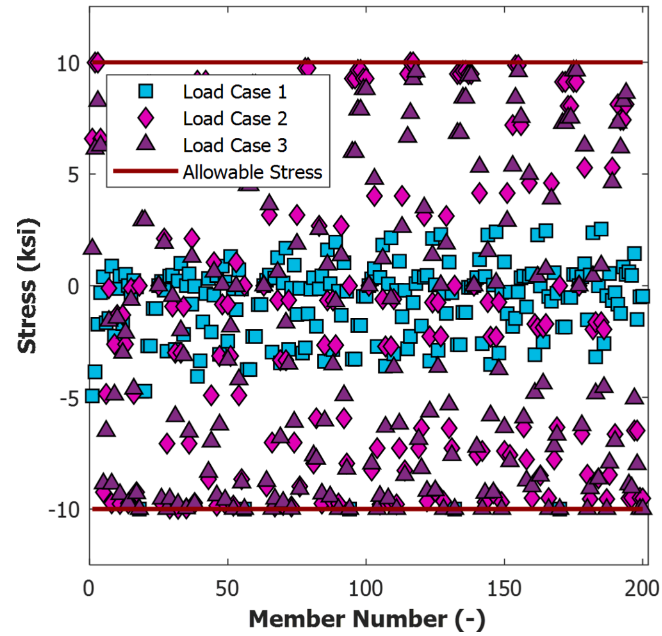

Fig. 16. Optimized result constraint values for the 200-bar truss structure.

investigated. It hence follows that the benchmark has 204 non-linear design constraints (44 tensile/compressive stress and 24 displacement constraints) accounting for each of the loading scenarios.

Table 8 lists and compares the results of other metaheuristic optimizers with the present work. Among feasibly produced designs, the PO algorithm obtained the best optimized weight (1023.89 Ib.) with the least amount of computational effort (8,976 structural analyses), where a total CPU time of 8.3 s was required for every optimization cycle. Fig. 9 shows the constraint boundaries estimated at the optimal solution by PO. It is evident from the figure that no stress (tensile/compressive) or displacement constraints were violated by the proposed design for all three loading scenarios. Lighter solutions reported by HS [10] and HPSO [6], upon closer investigation, were both found to violate pre-imposed design limitations by a factor of 0.008 and 4.217, respectively. Algorithms with feasible results that are comparable to PO such as HPSSO [28], WEO [20], EM-MS [45], and the Optics Inspired Optimizer (OIO) [45] were observed to be lacking in comparison either in computational efficiency or solution stability. This was found to be the case with infeasible designs as well. Considerably lower mean and standard deviation values for the 50 independent runs of the PO algorithm clearly demonstrates the robust algorithmic stability. This is in part due to the relaxed penalty function scheme adopted in this study as well as the excellent exploration–exploitation balance inherent to the algorithmic process itself.

4.4. Spatial 25-bar truss structure

The 25-bar spatial truss structure is geometrically shown in Fig. 10. All truss members are made of a material having a mass density of 0.1 Ib./in^3 and elastic modulus of 10,000 ksi. Since the tower is doubly symmetric about the x and y axis, structural members were grouped into eight independent design variables. The member groupings and their corresponding stress limitations are shown in Table 9. In adherence with literary trend, the minimum and maximum cross-sectional values for all members were set as $A_{min} = 0.01$ in^2 and $A_{max} = 3.4$ in^2, respectively. The allowable nodal displacements values for all free nodes were limited to ± 0.35*in* in the x, y, and z direction. Two loading conditions are considered for this problem and is shown in Table 10. As a whole, the benchmark has 124 non-linear design constraints (50 tensile/compressive stress and 12 displacement constraints) for each loading condition.

Table 11 lists a comparison of designs developed by the PO algorithm with other optimizations techniques. Final optimized design presented by PO clearly outperforms all other algorithms presented in literature either in final optimized weight, algorithmic stability, or convergence speeds. A total of 8,316 structural analyses was required for convergence and a CPU time of 5.3 s was recorded for a single optimization run. None of the normal stresses (tensile/compression) or nodal displacement values of the optimized design violated the pre-imposed design constraints. Fig. 11 graphically depicts this with most member stresses and nodal displacements values well below the upper and lower design constraint limits. Solutions that were found to be comparable to PO such as Bat Algorithm (BA) [29], HPSSO [28], and WEO [20], all required significantly more structural analyses. Quantitatively, the PO was estimated to be 58.42%, 37.59%, and 57.89% computationally more efficient than the above mentioned algorithms, respectively. It furthermore outperforms the results presented by ACO [7], HPSO [6], ABC-AP [8], the Cyclic Parthenogenesis Algorithm (CPA) [39], mTLBO [27], and the Plasma Generation Optimizer (PGO) [40] in terms of final optimized weight and convergence speeds by varying extents. Based on this comparison, an overall inference can be reached that the political optimizer algorithm is superior to most heuristic methods available in literature for the 25-bar truss structure.

4.5. Spatial 72-bar truss structure

The 72-bar spatial truss tower is schematically depicted in Fig. 12. By dint of structural radial symmetry, truss members were grouped into 16 independent design variables (Table 13). The structure was assumed to be constructed from the same material having a mass density of 0.1 Ib./in^3 and elastic modulus of 10,000 ksi. Normal member stresses were limited to 25 ksi for both tension and compression. Moreover, nodal displacement values in the upper-most nodes (*17, 18, 19, and 20*) were limited to ± 0.25*in* in the x and y direction. Two independent loading conditions, as shown in Table 12, were considered for the current problem. As a whole, the benchmark has 320 non-linear design constraints (72 tension/compression, and 16 displacement) that account for each of the two loading scenarios.

Finally, for the purpose of a more comprehensive investigation, two versions of the benchmark that exist in literature were presented in this section. Case 1 involves a minimum cross-sectional value of $A_{min} = 0.1$

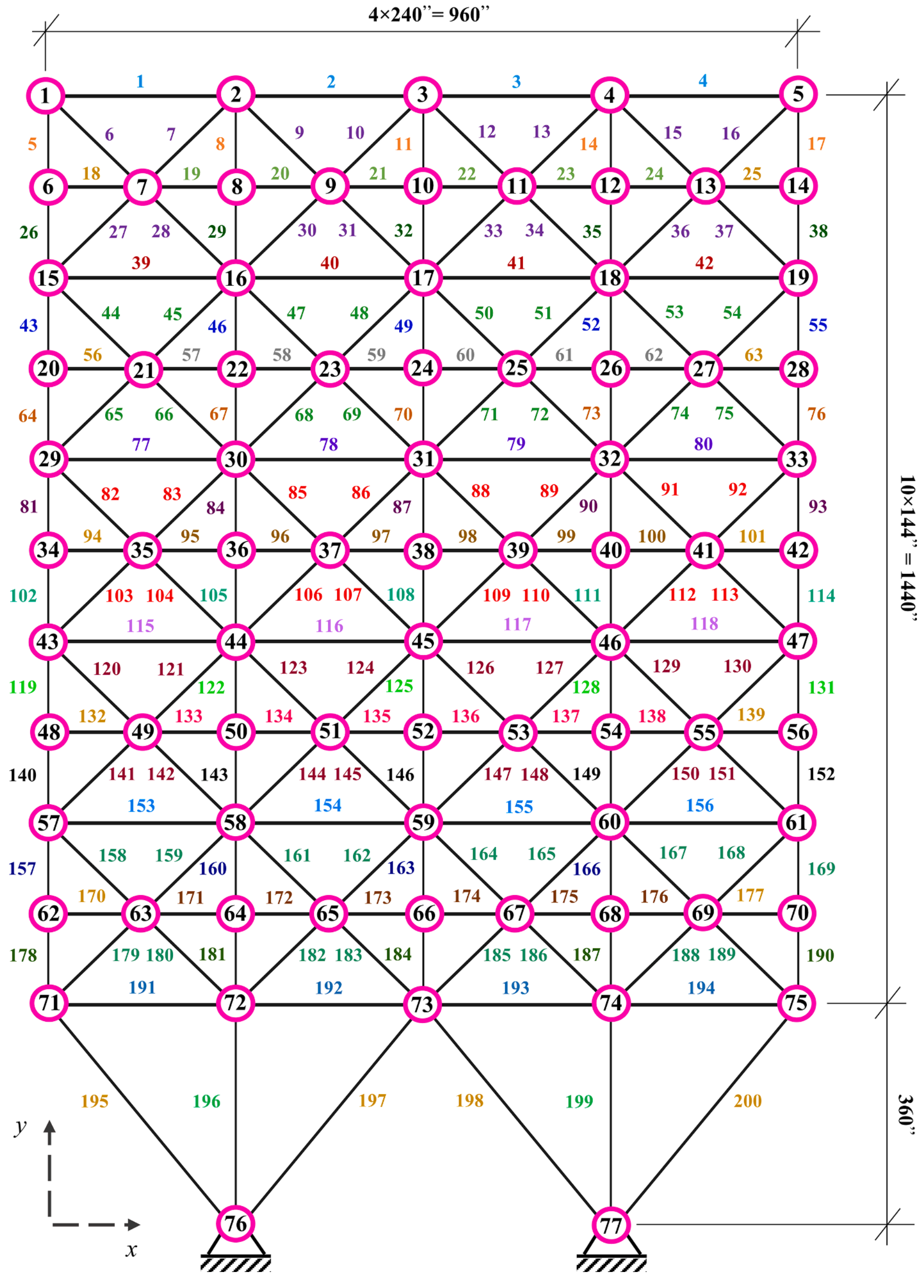

Fig. 17. Schematic for the 200-bar planar truss.

in^2 and Case 2 has an assigned minimum value of $A_{min} = 0.01$ in^2. For both cases, a maximum design variable (A_{max}) value of 4.0 in^2 was employed during the entire optimization process.

A summary of the results obtained by the PO algorithm along with other optimization methods reported in literature are presented in Tables 14 and 15. Among tabulated results, the proposed algorithm produced the lightest design of 379.68 Ib and 363.88 Ib in 7,788 and 8,448 structural analyses for cases 1 and 2, respectively. It is evident that no other algorithm outperformed PO in terms of either solution quality or speed. Moreover, with regards to solution stability, the mean and standard deviation of 50 runs for the PO algorithm proved to be superior (lower) than all metaheuristics presented in literature. Owing to algorithm's efficient population partitioning scheme and relaxed fitness function penalization strategy, variation in final solution values were kept to a minimum, all the while ensuring best possible results. The only study comparable to PO, in terms of computational efficiency, was the Hybrid Elephant Herding-Cultural Optimizer Algorithm (EHOC) proposed by Malihe *et al.* [46] for case 1 of the benchmark. Nevertheless, final structural weight produced by the algorithm (379.72 Ibs.) was found to be heavier than PO. Fig. 15 shows the convergence curve of the PO algorithm for both cases of the 72-bar truss structure. Figs. 13 and 14 show the normalized constraint values for the optimized designs. No constraint violations have been recorded and a total CPU time of 64 s was necessary to reach convergence.

Video 1 shows a sample optimization animated plot for case 1 of the 72-bar truss. Since the population of search agents is the same for all benchmarks, a total of 121 party members are actively involved in searching for the global optimum. Every frame of the animation, displays the best solution found in every current iteration. Variable member thickness corresponds to larger cross-sectional areas and is related to one another by means of a predefined weight factor.

Table 16
Element grouping for the 200-bar planar truss.

Design Variable	Member Grouping	Design Variable	Member Grouping
A_1	1, 2, 3, 4	A_{16}	82, 83, 85, 86, 88, 89, 91, 92, 103, 104, 106, 107, 109,110, 112, 113
A_2	5, 8, 11, 14, 17	A_{17}	115, 116, 117, 118
A_3	19, 20, 21, 22, 23, 24	A_{18}	119, 122, 125, 128, 131
A_4	18, 25, 56, 63, 94, 101, 132, 139, 170, 177	A_{19}	133, 134, 135, 136, 137, 138
A_5	26, 29, 32, 35, 38	A_{20}	140, 143, 146, 149, 152
A_6	6, 7, 9, 10, 12, 13, 15, 16, 27, 28, 30, 31, 33, 34, 36, 37	A_{21}	120, 121, 123, 124, 126, 127, 129, 130, 141, 142,144, 145, 147, 148, 150, 151
A_7	39, 40, 41, 42	A_{22}	153, 154, 155, 156
A_8	43, 46, 49, 52, 55	A_{23}	157, 160, 163, 166, 169
A_9	57, 58, 59, 60, 61, 62	A_{24}	171, 172, 173, 174, 175, 176
A_{10}	64, 67, 70, 73, 76	A_{25}	178, 181, 184, 187, 190
A_{11}	44, 45, 47, 48, 50, 51, 53, 54, 65, 66, 68, 69, 71, 72, 74, 75	A_{26}	158, 159, 161, 162, 164, 165, 167, 168, 179, 180,182, 183, 185, 186, 188, 189
A_{12}	77, 78, 79, 80	A_{27}	191, 192, 193, 194
A_{13}	81, 84, 87, 90, 93	A_{28}	195, 197, 198, 200
A_{14}	95, 96, 97, 98, 99, 100	A_{29}	196, 199
A_{15}	102, 105, 108, 111, 114		

4.6. A 200-bar planar truss structure

To investigate PO efficiency at optimizing larger structural systems, the 200-bar planar truss structure has been chosen for optimization (Fig. 17). The structure has been previously investigated by Lee and Geem [10], Sonmez [8], Degertekin [15], Dede and Ayvaz [51], Kaveh and Zakian [49], Kaveh and Bakhshpoori [20], among others. Members are grouped into 29 independent design variables and are linked together as shown in Table 16. The modulus of elasticity and material density of all members were set as 30,000 ksi and 0.283 Ib./in^3, respectively. Allowable member stresses for both tension and compression were limited to 10 ksi. No nodal displacement limitations were imposed. The minimum and maximum cross-sectional area values for all load bearing members were set to $A_{min} = 0.1$ in^2 and $A_{max} = 20.0$ in^2. Three independent loading scenarios were considered: **(1)** 1.0 kip acting in the positive x-direction at nodes 1, 6, 15, 20, 29, 34, 43, 48, 57, 62 and 71; **(2)** 10.0 kips acting in the negative y-direction at nodes 1, 2, 3, 4, 5, 6, 8, 10, 12, 14, 15, 16, 17, 18, 19, 20, 22, 24, 26, 28, 29, 30, 31, 32, 33, 34, 36, 38, 40, 42, 43, 44, 45, 46, 47, 48, 50, 52, 54, 56, 57, 58, 59, 60, 61, 62, 64, 66, 68, 70, 71, 72, 73, 74 and 75; **(3)** loading conditions (1) and (2) acting together. The problem, therefore, has a total of 1200 nonlinear constraints (200 tension and 200 compression, for each of the loading scenarios).

Table 17 compares the designs developed by the PO algorithm among others previously reported in literature. Due to the large number of design variables involved, considerable variations in optimized results are immediately manifest. A quick comparison among tabulated solutions clearly show the advantage that the PO algorithm has over other previously proposed techniques for the 200-bar truss. A final weight of 25,479.6 Ib was obtained in 27,984 structural analyses with a computational time of 112 s. This proposed optimized structure is, by far, the lightest among all tabulated solutions presented. Where convergence speeds are concerned, it was found that SFLA [52], IWO [52], SFLA-IWO [52], Improved Grey Wolf Optimizer (IGWO) [49], and WEO [20] were all less computationally taxing. This, however, comes at a price since the final designs presented by these algorithms were considerably larger. The only aspect where the PO algorithm seems to be at a disadvantage in comparison to others was in regards to algorithmic stability. Solution stability and robustness of the PO algorithm was quantified based on the mean weight and standard deviation of 50 independent runs. A slightly higher standard deviation value compared with some of the other metaheuristics (TLBO, CPA, ACCS, and SFLA-IWO) for the PO algorithm underscores the reduced solution robustness that the optimization method inherently harbors for large sized structures. Simultaneously, however, the PO algorithmic stability outperformed all other remaining modern metaheuristic algorithms. Fig. 16 shows all member stresses conforming to the predefined constraint values mentioned earlier for all three loading conditions at the optimized design and Video 2 presents an animation of the 200-bar optimization history.

4.7. A 26-Storey 942-bar truss tower

The final example considered in this study is that of a 26-storey 942-bar truss tower schematically depicted in Fig. 18. A considerable body of literature optimizes the structure to demonstrate the ability of solution methodologies at handling real-sized structures. Two versions of the benchmark exist. The first uses discrete section areas as design variables, while the second adopts continuous ones. In the present work, the continuous version of the structure will be considered and upper/lower design variable bounds of 0.1 and 200 in^2, respectively, has been taken. Further details regarding member grouping and design constraints can be found in reference [54].

The results obtained by PO and other existing optimization techniques are compared in Table 18. Fig. 19 shows the existing member stresses and nodal displacement values at the optimum design. As clearly shown, none of the pre-imposed design constraints have been violated. Final optimized weight obtained by PO was found to be 133,831.96 lb. which is the best among optimized results in literature. The algorithm that came closest to PO with regards to weight was with Cuckoo Search algorithm (134,119.6 Ib.) implemented by Gandomi *et al.* [58]. Furthermore, in terms of convergence speeds, the PO algorithm required the least amount of computational effort (24,420 structural analysis) when compared to other methods and had a total CPU time of 350 s per run. This primarily is owed to the PO's exceptional exploration strategy (sub-population and shuffling scheme) which facilitates the algorithm in escaping from local optima quickly. Moreover, low penalization factors for the objective function encourages the algorithm to explore, as much as possible, the feasible-infeasible border regions where global optimum values are usually found.

The only aspect in which the PO algorithm seems to be slightly lacking is with algorithmic solution stability. This was evident for all of the larger trusses investigated in this study, and the 942-bar benchmark was found to be no exception. Slightly larger standard deviation and mean values for the 50 independent runs in comparison to other optimizers in literature is immediately manifest from Table 18. Nevertheless, this decreased solution accuracy for PO is within acceptable limits and does not seriously compromise the inherent strength and robustness of the algorithm as a structural optimizer. Fig. 20 illustrates all final results of the 50 independent runs conducted by PO. Most of the runs are shown to be confined within the minimum and average weights limits. This illustrates that despite larger numerical values of standard deviation, the algorithm is expected to perform reasonably well for most optimization runs. In that sense, the PO algorithm is strongly recommended as a structural optimizer capable of dealing with small or large structures with multiple loading and design constraints.

5. Discussion of PO structural optimization efficiency

Based off optimized solutions presented earlier, the PO algorithm has proven to be a robust and overall versatile structural optimization metaheuristic capable of effectively dealing with small and large truss systems alike. Key reasons for this can be conveniently cited/summarized as follows:

(a) *Dual Population Partitioning Scheme*: As mentioned already at the outset of this study, the PO algorithm adopts the "multi-

Table 17
Optimized results for the 200-bar planar truss.

Design variable (in^2)	Toğan & Daloğlu [53] (GA)	Sonmez [8] (ABC-AP)	Degertekin & Hayalioglu [15] (TLBO)	Kaveh & Bakhshpoori [20] (WEO)	Kaveh & Zolghadr [39] (CPA)	Kaveh & Zakian [49]		Kooshkbaghi & Kaveh [21] (ACCS)	Kaveh *et al.* [52]			Ozbasaran & Yildirim [50]		This study (PO)
						(GWO)	(IGWO)		(SFLA)	(IWO)	(SFLA-IWO)	(CSA)	(mCSA)	
A_1	0.3469	0.1039	0.146	0.1144	0.1721	1.3363	0.1024	0.127	0.1553	1.7400	0.1291	0.6244	0.1123	0.13911
A_2	1.0810	0.9463	0.941	0.9443	0.9553	2.7525	0.9654	0.954	1.4015	11.5591	0.9551	1.2710	4.0640	0.96277
A_3	0.1000	0.1037	0.100	0.1310	0.1000	0.5923	0.1391	0.122	0.1271	5.4086	0.1367	2.9828	5.2336	0.10996
A_4	0.1000	0.1126	0.101	0.1016	0.1004	0.5258	0.1741	0.1	0.2324	0.1303	0.1007	1.1929	1.4436	0.1
A_5	2.1421	1.9520	1.941	2.0353	1.9662	5.0281	1.9613	1.968	1.9778	3.1979	1.9405	1.9144	3.0197	1.943
A_6	0.3470	0.2930	0.296	0.3126	0.3055	0.4945	0.2899	0.293	0.2832	0.1364	0.3012	0.2686	0.1098	0.29526
A_7	0.1000	0.1064	0.100	0.1679	0.1000	1.7505	0.1294	0.115	0.2435	5.2513	0.1050	0.5046	7.1450	0.10006
A_8	3.5650	3.1249	3.121	3.1541	3.1618	3.3725	3.1511	3.095	3.1891	2.9932	3.1091	2.9974	13.5230	3.0987
A_9	0.3470	0.1077	0.100	0.1003	0.1152	0.2057	0.1251	0.103	0.1010	2.2177	0.1129	6.7782	2.5863	0.13761
A_{10}	4.8050	4.1286	4.173	4.1005	4.2405	4.3035	4.0627	4.094	4.2345	3.8558	4.1090	17.2577	7.5748	4.0992
A_{11}	0.4400	0.4250	0.401	0.4350	0.4046	0.7077	0.4131	0.41	0.4942	0.5493	0.4145	0.6154	0.2710	0.41926
A_{12}	0.4400	0.1046	0.181	0.1148	0.1000	0.1212	0.4043	0.152	0.6314	10.3265	0.1197	0.1836	0.2109	0.15592
A_{13}	5.9520	5.4803	5.423	5.3823	5.4132	6.6465	5.3357	5.393	5.4556	7.6522	5.4226	12.0539	5.1189	5.4344
A_{14}	0.3470	0.1060	0.100	0.1607	0.1545	0.1000	0.2632	0.198	0.4106	0.6086	0.1843	3.1875	0.1054	0.10437
A_{15}	6.5720	6.4853	6.422	6.4152	6.3976	6.9236	6.3226	6.395	6.3062	6.1152	6.4222	5.8229	8.8993	6.4355
A_{16}	0.9540	0.5600	0.571	0.5629	0.5555	0.8096	0.7972	0.597	0.9972	1.2809	0.5826	1.3869	0.4816	0.56508
A_{17}	0.3470	0.1825	0.156	0.4010	0.4425	0.1943	0.1791	0.106	0.3502	0.3930	0.1370	0.1262	2.7967	0.15753
A_{18}	8.5250	8.0445	7.958	7.9735	8.0928	7.9800	8.1268	7.99	8.1519	14.4101	7.9800	7.5369	9.4103	7.9672
A_{19}	0.1000	0.1026	0.100	0.1092	0.1004	0.9110	0.1141	0.103	0.9147	0.1564	0.1110	2.3128	0.5145	0.10012
A_{20}	9.3000	9.0334	8.958	9.0155	8.9918	10.7262	9.1337	8.987	9.0237	9.5304	8.9783	12.8093	8.4612	8.9675
A_{21}	0.9540	0.7844	0.720	0.8628	0.8925	1.0542	0.8000	0.692	1.3172	0.8674	0.7307	0.6470	1.1859	0.72223
A_{22}	1.7639	0.7506	0.478	0.2220	0.2544	0.2809	0.2487	0.142	0.4441	2.3461	0.4531	12.8362	0.1805	0.48433
A_{23}	13.3006	11.3057	10.897	11.0254	11.1214	15.0000	11.2008	10.747	12.4237	13.6192	10.9215	8.8380	10.9687	10.913
A_{24}	0.3470	0.2208	0.100	0.1397	0.1000	0.1310	0.1136	0.101	0.2864	0.1804	0.2607	7.3364	7.5644	0.10472
A_{25}	13.3006	12.2730	11.897	12.0340	12.3304	15.0000	12.1703	11.747	13.6510	13.8236	11.9207	9.8124	12.3189	11.914
A_{26}	2.1421	1.4055	1.080	1.0043	1.0110	0.9469	0.9947	0.834	1.5028	1.9525	1.1723	6.0571	2.3043	1.0842
A_{27}	4.8050	5.1600	6.462	6.5762	6.4103	7.8886	6.3377	7.452	4.8959	3.5929	6.3036	3.0232	9.0358	6.5093
A_{28}	9.3000	9.9930	10.799	10.7265	10.5814	15.0000	10.5338	11.169	9.1316	8.5786	10.6357	8.5791	10.0101	10.7
A_{29}	17.1740	14.70144	13.922	13.9666	14.1288	13.8801	14.0917	13.482	15.9098	16.6203	14.0674	18.3325	15.0433	13.952
Weight **(Ib)**	**28,544.0**	**25,533.79**	**25,488.15**	**25,674.83**	**25,651.58**	**33,137.452**	**25,771.78**	**25,481.45**	**27,480.16**	**27,103.16**	**25,544.11**	**41,628.8**	**37,691.49**	**25,479.67**
Mean **(Ib)**	N/A	N/A	25,533.14	26,613.45	25957.15	34,561.68	26,699.19	25,527.66	29,420.11	28,924.08	25,774.51	51,936.32	41,797.75	25,614.23
Stdev **(Ib)**	N/A	N/A	27.44	702.80	254.06	991.9221	410.4016	25.49	1723.39	15,454.86	254.1263	4602.07	2663.91	376.11
CV (−)	**None**	**None**	**None**	**None**	**None**	**None**	**None**	**None**	**None**	**None**	$\mathbf{0.13 \times 10^{-3}}$	**None**	**None**	**None**
NSA	**51,360**	**1,450,000**	**28,059**	**19,410**	**34,560**	**13,200**	**23,760**	**45,000**	**16,000**	**16,000**	**18,000**	**150,000**	**150,000**	**27,984**

Note: 1 in^{-2} = 6.452 cm^2; 1 lb. = 4.45 N.

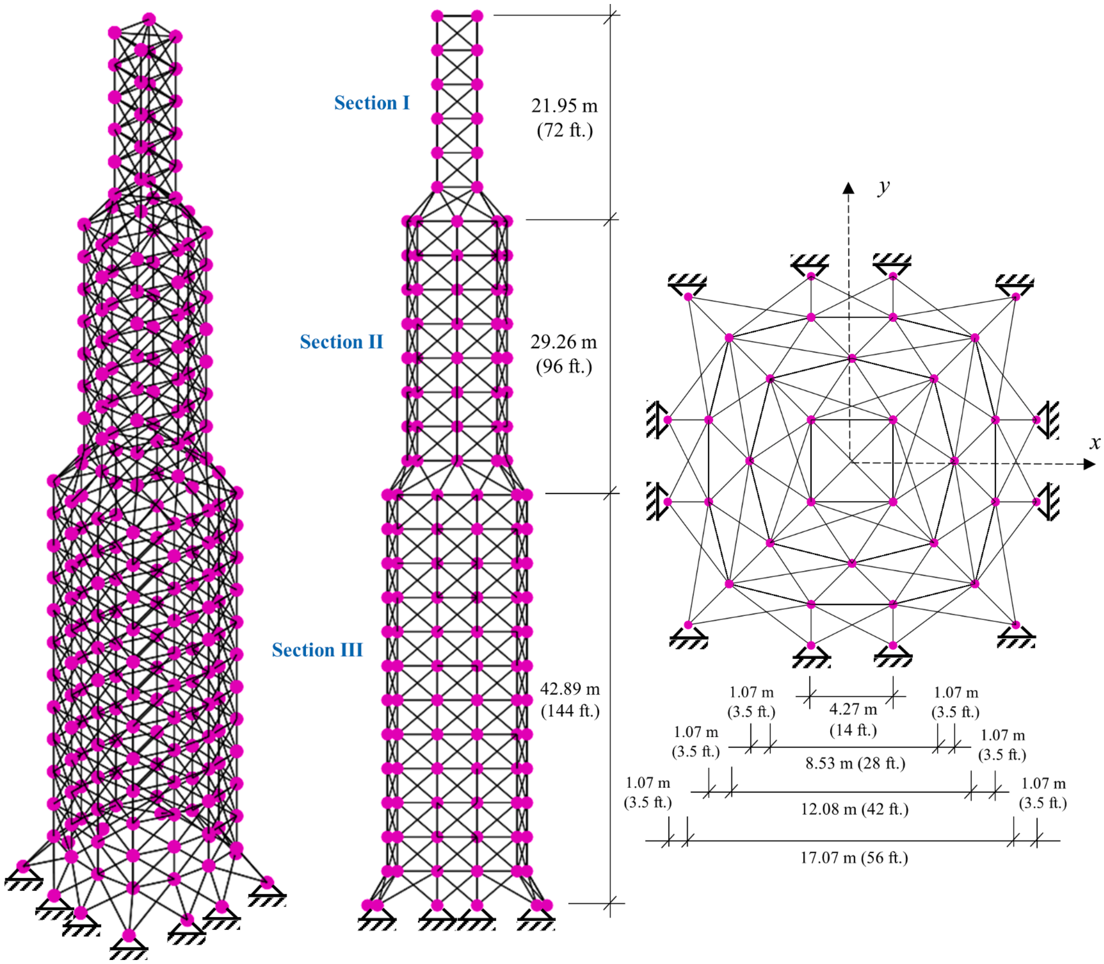

Fig. 18. Schematic of the 942-bar truss tower (a) Isometric View (b) Front View (c) Top View.

population" strategy to enhance exploration and avoid getting snarled in local optima. By dividing the population into political parties and subsequently electoral districts (constituencies), the PO algorithm was able to obtain the lightest truss designs with the least amount of computational effort for both small and large scale structures. Truss sizing problems inherently have challenging search landscapes and it seems that adopting this strategy serves as an additional exploration boost.

(b) *Novel Exploitation Method*: By adopting the RPPUS [32] exploitation method, promising solution regions were exploited effectively by the algorithm. One of the main advantages of this method is the updating of each dimension of the design variable independently either with local party leaders or constituency winners. This is especially useful in truss sizing problems where each dimension represented a single design group. Furthermore, search agents adopted a collective swarm-like behavior seeking better designs and avoiding poorer ones.

(c) *Relaxed Penalty Factors*: In order to fully exploit the inherent strength of the PO algorithm, penalization of near feasible truss designs was required to be kept to a minimum during the initial exploration phase. A relaxed penalty objective function formulation [36] was adopt for this purpose. Metaheuristic algorithms are primarily designed to deal with unconstrained design problems. By reducing the amount of penalization, speed and accuracy of the PO algorithm was dramatically enhanced in comparison if more traditional static penalty function method were adopted.

Finally, it was observed that for the small/medium sized truss systems (10-bar, 18-bar, 22-bar, 25-bar, and 72-bar trusses) the PO algorithm performed exceptionally well in terms of final weight, convergence speeds, and solution stability when compared with previous studies. For large-scale structural systems (200-bar and 942-bar), however, a noticeable, yet acceptable degree of algorithmic instability was found in comparison with other algorithms. The author may possibly attribute this behavior to the fact that the PO performance parameters (N and λ), used throughout this study, were initially fine-tuned for the small-scale 10-bar planar truss benchmark. This could have had an effect on the final results for larger truss structures. Future studies need to verify this by either performing an independent sensitivity analysis exclusively for large-scale structures or attempt to adjust the upper limit of iterations per optimization run.

6. Conclusion

In this study, a formal investigation into the robustness and feasibility of the recently proposed political optimizer algorithm in structural optimization with continuous sizing variables has been presented. A number of classical benchmark truss structures in both planar and spatial domains, subjected to multiple loading conditions and design constraints, have been employed to demonstrate the efficacy of the proposed technique. To showcase the potential applicability of the PO algorithm at optimizing real-sized structures, two large-scale truss structural systems (200-bar and 942-bar tower) were chosen for this purpose.

Owing to its robust exploration–exploitation capabilities and multi-

Table 18
Optimized results for the 26-Storey 942-bar truss tower.

Design variable (in^2)	Hasançebi & Erbatur [55] (SA)	Hasançebi [56] (ES)	Rahami et al. [57] (GNMS)	Talatahari et al. [14] (FA)	Gandomi et al. [58] (CS)	Kaveh & Zakian [49]		Degertekin et al. [59] (JA)	Cao et al. [54]		This study (PO)
						(GWO)	(IGWO)		(FPA)	(TLBO)	
A_1	1	1.02	2.786	N/A	1	1.4245	4.2489	1.045258	8	22	1
A_2	1	1.037	1.357	N/A	1	2.1232	1.7702	1.001630	5	46	1.0180
A_3	3	2.943	5.036	N/A	3.01	2.1749	1.5892	3.549999	9	141	3.6539
A_4	1	1.92	2.24	N/A	1.75	2.3746	1.5235	1.924590	3	42	1.9956
A_5	1	1.025	1.223	N/A	1	1.0000	1.0265	1.000032	3	31	1.1953
A_6	17	14.961	14.958	N/A	14.27	17.5705	15.3979	15.337079	16	32	14.3010
A_7	3	3.074	2.957	N/A	2.93	3.3655	2.8825	3.108905	4	1	2.6488
A_8	7	6.78	10.904	N/A	1	19.1722	6.9912	6.589077	15	40	3.2394
A_9	20	18.58	14.418	N/A	1	12.8837	11.2039	16.569661	20	119	5.2759
A_{10}	1	2.415	3.709	N/A	9.38	2.6161	2.7262	2.553777	4	59	7.9579
A_{11}	8	6.584	5.708	N/A	4.43	3.9268	8.1921	6.433946	5	1	7.1826
A_{12}	7	6.291	4.926	N/A	4.54	4.7984	6.2178	5.812166	6	1	7.1283
A_{13}	19	15.383	14.175	N/A	16.41	12.4939	16.5585	15.836882	19	7	16.5762
A_{14}	2	2.1	1.904	N/A	2.33	1.0000	2.3668	2.196943	2	73	2.2929
A_{15}	5	6.021	2.81	N/A	7.51	1.6022	4.1519	4.324553	9	42	4.3833
A_{16}	1	1.022	1	N/A	1	1.0000	1.2370	1.000047	2	39	1.0109
A_{17}	22	23.099	18.807	N/A	22.47	16.8974	22.3006	21.973772	13	145	20.2929
A_{18}	3	2.889	2.615	N/A	2.7	2.5670	2.9996	2.674909	2	1	2.9265
A_{19}	9	7.96	12.533	N/A	13.58	6.3981	7.7559	8.722646	14	47	8.7818
A_{20}	1	1.008	1.131	N/A	1	1.1522	1.1283	1.000032	1	7	1.0511
A_{21}	34	28.548	30.512	N/A	28.93	29.0131	28.2646	29.898613	18	8	28.2137
A_{22}	3	3.349	3.346	N/A	3.23	3.5656	3.1924	3.249223	3	96	3.2527
A_{23}	19	16.144	17.045	N/A	23.87	17.4563	16.3965	16.995624	19	40	14.7304
A_{24}	27	24.822	18.079	N/A	41.67	21.3364	22.6095	25.510407	23	28	27.9577
A_{25}	42	38.401	39.272	N/A	36.02	19.0983	40.0759	37.634066	55	1	38.9819
A_{26}	1	3.787	2.606	N/A	6.41	11.6687	5.3549	1.220731	1	89	1.9847
A_{27}	12	12.32	9.83	N/A	23.79	7.2854	9.2695	11.944077	14	28	12.1569
A_{28}	16	17.036	13.113	N/A	28.39	13.2728	15.0911	16.515003	16	83	16.6744
A_{29}	19	14.733	13.69	N/A	19.38	10.9616	14.0704	14.822892	17	11	14.5231
A_{30}	14	15.031	16.978	N/A	20.31	16.9994	15.1962	15.983565	14	120	14.1466
A_{31}	42	38.597	37.601	N/A	31.41	51.2551	37.1490	38.514252	29	27	33.4677
A_{32}	4	3.511	3.06	N/A	2.57	3.5553	3.1643	3.323571	4	37	3.1529
A_{33}	4	2.997	5.511	N/A	4.18	10.7749	3.4414	3.189674	5	1	2.7595
A_{34}	4	3.06	1.801	N/A	3.33	2.2552	2.2813	2.822370	5	46	2.7334
A_{35}	1	1.086	1.157	N/A	1	2.8847	1.0166	1.001323	1	20	1.0041
A_{36}	1	1.462	1.242	N/A	1	1.4999	1.4089	1.002606	3	144	1.0375
A_{37}	62	59.433	62.774	N/A	47.11	74.8387	59.6649	59.530117	44	41	57.0798
A_{38}	3	3.632	3.328	N/A	2.35	4.4502	3.3173	3.250054	3	2	2.9917
A_{39}	2	1.887	4.237	N/A	3.79	4.5565	2.0249	2.068093	5	21	2.0256
A_{40}	4	4.072	1.72	N/A	3.3	1.6472	2.3953	3.084539	3	80	2.8508
A_{41}	1	1.595	1.015	N/A	1	1.6962	1.0554	1.000717	2	1	1.1657
A_{42}	2	3.671	5.643	N/A	1	1.0000	1.2294	1.239938	2	107	1.3137
A_{43}	77	79.511	78.009	N/A	63.33	72.9916	79.5798	79.891179	63	138	72.1009
A_{44}	3	3.394	3.221	N/A	3.21	3.3433	3.2875	3.299488	3	38	3.1772
A_{45}	2	1.581	3.593	N/A	4.86	1.9913	1.9028	1.964128	3	74	1.8702
A_{46}	3	4.204	4.767	N/A	2.22	2.3226	3.2460	3.489718	4	12	3.3290
A_{47}	2	1.329	1.153	N/A	1	1.1452	1.0277	1.000032	4	84	1.0984
A_{48}	3	2.242	2.17	N/A	1	1.0000	1.0898	1.000032	2	99	1.0462
A_{49}	100	96.886	99.641	N/A	76.93	96.6037	93.8836	97.181471	72	40	92.7197
A_{50}	4	3.71	4.147	N/A	3.54	4.0309	3.0634	3.322281	4	16	3.3618
A_{51}	1	1.055	2.16	N/A	3.91	1.8735	1.7246	1.002997	6	154	1.2291
A_{52}	4	4.566	4.15	N/A	2.25	4.7339	3.9313	3.651629	5	4	3.1938
A_{53}	6	9.606	11.207	N/A	11.44	10.6370	8.1063	7.226228	26	16	11.0260
A_{54}	3	2.984	11.09	N/A	11.64	3.4612	9.8391	4.544599	38	106	8.8411
A_{55}	49	45.917	35.95	N/A	36.94	44.5447	42.7529	41.411074	53	80	40.1639
A_{56}	1	1	2.194	N/A	1	1.2428	1.1219	1.002207	1	1	1.0071
A_{57}	62	62.426	66.171	N/A	48.1	76.1124	63.0179	64.803517	35	47	61.5728
A_{58}	1	2.977	3.34	N/A	5.88	11.4119	2.6542	2.525618	13	44	3.4131
A_{59}	3	1	4.053	N/A	1	4.7082	1.6685	1.000054	4	52	1.3026
Weight **(Ib)**	**143,436**	**141,241**	**142,296**	**138,878**	**134,119.6**	**147,841.7416**	**136,311.1322**	**137,344.356**	**139,589.3**	**781,697.1**	**133,831.96**
Mean **(Ib)**	N/A	N/A	N/A	139,682	135,244.7	165,168.9424	137,453.6697	137,379.616	N/A	N/A	139,794.652
Stdev **(Ib)**	N/A	N/A	N/A	1098	1497.06	5392.7272	673.8566	38.346	N/A	N/A	5904.70
CV (–)	**None**	**None**	**None**	**None**	**0.3797**	**None**	**None**	**None**	**None**	**None**	**None**
NSA	39,834	**150,000**	N/A	**50,000**	**75,000**	**28,000**	**28,000**	**58,274**	**30,263**	**61,566**	**24,420**

Note: 1 in^{-2} = 6.452 cm^2; 1 lb. = 4.45 N.

population scheme, the algorithm achieves convergence at near optimal solutions relatively early in the optimization process. Unlike most human behavior-based metaheuristics, the political optimizer contains only a few search parameters that require tuning prior any optimization task. These factors and more have encouraged the implementation of the proposed technique in the sizing of structural systems.

In conclusion, it is safe to surmise that the potential promise of the algorithm can be extended to not just structural sizing problems, but to truss topology and shape optimization in both discrete/continuous domains with static and dynamic loading conditions. It is recommended

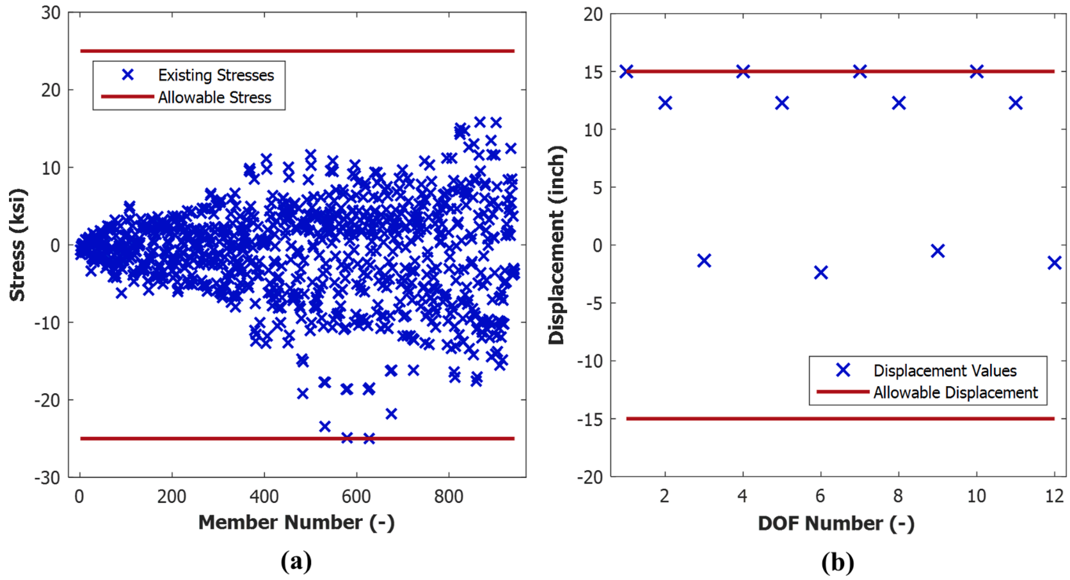

Fig. 19. Optimized result constraint values boundaries for the 942-bar truss tower (a) Stress constraint values (b) Displacement constraint values.

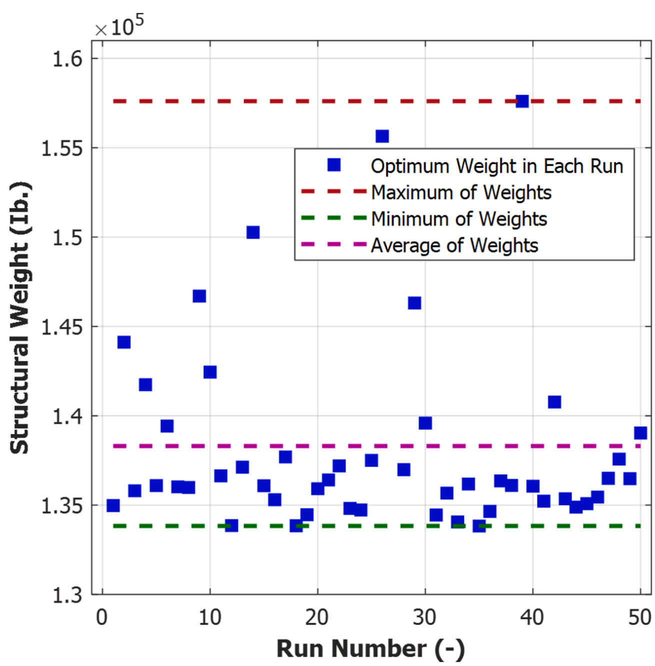

Fig. 20. The obtained structural weight in each independent run for the 942-bar truss tower.

that a formal investigation into the algorithm's robustness and stability be further established by implementing the PO technique in a number of other engineering applications, including plates, shells and frame optimization. Moreover, possible future enhancements to the inner working of the algorithm can be achieved by either adjusting certain mathematical formulations in the local or global search phases or hybridizing the technique with other metaheuristic or numerical methods.

Declaration of Competing Interest

The authors declare that they have no known competing financial interests or personal relationships that could have appeared to influence the work reported in this paper.

Acknowledgements

The author wishes to express his sincerest gratitude to Assistant Prof. Dr. Qamar Askari—GIFT University, Gujranwala, Pakistan, for his role in providing further information regarding the "party switching" phase of the algorithm and the anonymous reviewers for their careful reading and constructive feedback.

Appendix A. Supplementary data

Supplementary data to this article can be found online at https://doi.org/10.1016/j.istruc.2021.07.027.

References

[1] Wolpert DH, Macready WG. No free lunch theorems for optimization. IEEE Trans. Evol Comput 1997;1(1):67–82. https://doi.org/10.1109/4235.585893.

[2] Rajeev S, Krishnamoorthy CS. Discrete Optimization of Structures Using Genetic Algorithms. J Struct Eng 1992;118(5):1233–50. https://doi.org/10.1061/(ASCE)0733-9445(1992)118:5(1233).

[3] Cao G. Optimized design of framed structures using a genetic algorithm. Ph.D. thesis. The University of Memphis; 1996.

[4] Fourie PC, Groenwold AA. The particle swarm optimization algorithm in size and shape optimization. Struct Multidiscip Optim 2002;23(4):259–67. https://doi.org/10.1007/s00158-002-0188-0.

[5] Schutte JF, Groenwold AA. Sizing design of truss structures using particle swarms. Struct Multidiscip Optim 2003;25(4):261–9. https://doi.org/10.1007/s00158-003-0316-5.

[6] Li LJ, Huang ZB, Liu F, Wu QH. A heuristic particle swarm optimizer for optimization of pin connected structures. Comput Struct 2007;85(7-8):340–9. https://doi.org/10.1016/j.compstruc.2006.11.020.

[7] Camp CV, Bichon BJ. Design of Space Trusses Using Ant Colony Optimization. J Struct Eng 2004;130(5):741–51. https://doi.org/10.1061/(ASCE)0733-9445(2004)130:5(741).

[8] Sonmez M. Artificial Bee Colony algorithm for optimization of truss structures. Appl. Soft Comput. J., vol. 11, Elsevier B.V.; 2011, p. 2406–18. https://doi.org/10.1016/j.asoc.2010.09.003.

[9] Sonmez M. Discrete optimum design of truss structures using artificial bee colony algorithm. Struct Multidiscip Optim 2011;43(1):85–97. https://doi.org/10.1007/s00158-010-0551-5.

[10] Lee KS, Geem ZW. A new structural optimization method based on the harmony search algorithm. Comput Struct 2004;82(9-10):781–98. https://doi.org/10.1016/j.compstruc.2004.01.002.

[11] Erol OK, Eksin I. A new optimization method: Big Bang-Big Crunch. Adv Eng Softw 2006;37(2):106–11. https://doi.org/10.1016/j.advengsoft.2005.04.005.

[12] Camp CV. Design of Space Trusses Using Big Bang-Big Crunch Optimization. J Struct Eng 2007;133(7):999–1008. https://doi.org/10.1061/(ASCE)0733-9445(2007)133:7(999).

[13] Yang XS. Firefly algorithms for multimodal optimization. Lect Notes Comput Sci 2009;5792 LNCS:169–78. https://doi.org/10.1007/978-3-642-04944-6_14.

[14] Talatahari S, Gandomi AH, Yun GJ. Optimum design of tower structures using Firefly Algorithm. Struct Des Tall Spec Build 2014;23(5):350–61. https://doi.org/10.1002/tal.v23.510.1002/tal.1043.
[15] Degertekin SO, Hayalioglu MS. Sizing truss structures using teaching-learning-based optimization. Comput Struct 2013;119:177–88. https://doi.org/10.1016/j.compstruc.2012.12.011.
[16] Rao RV, Savsani VJ, Vakharia DP. Teaching-learning-based optimization: A novel method for constrained mechanical design optimization problems. CAD Comput Aided Des 2011;43(3):303–15. https://doi.org/10.1016/j.cad.2010.12.015.
[17] Kaveh A, Mahdavi VR. Colliding Bodies Optimization method for optimum design of truss structures with continuous variables. Adv Eng Softw 2014;70:1–12. https://doi.org/10.1016/j.advengsoft.2014.01.002.
[18] Bekdaş G, Nigdeli SM, Yang XS. Sizing optimization of truss structures using flower pollination algorithm. Appl Soft Comput J 2015;37:322–31. https://doi.org/10.1016/j.asoc.2015.08.037.
[19] Yang XS. Flower pollination algorithm for global optimization. Lect Notes Comput Sci 2012;7445 LNCS:240–9. https://doi.org/10.1007/978-3-642-32894-7_27.
[20] Kaveh A, Bakhshpoori T. A new metaheuristic for continuous structural optimization: water evaporation optimization. Struct Multidiscip Optim 2016;54(1):23–43. https://doi.org/10.1007/s00158-015-1396-8.
[21] Kooshkbaghi M, Kaveh A. Sizing Optimization of Truss Structures with Continuous Variables by Artificial Coronary Circulation System Algorithm. Iran J Sci Technol - Trans. Civ Eng 2020;44(1):1–20. https://doi.org/10.1007/s40996-019-00254-2.
[22] Kaveh A, Aghakouchak AA, Zakian P. Reduced record method for efficient time history dynamic analysis and optimal design. Earthq Struct 2015;8:639–63. https://doi.org/10.12989/eas.2015.8.3.639.
[23] Zakian P. Meta-heuristic design optimization of steel moment resisting frames subjected to natural frequency constraints. Adv Eng Softw 2019;135:102686. https://doi.org/10.1016/j.advengsoft.2019.102686.
[24] Zakian P, Ordoubadi B, Alavi E. Optimal design of steel pipe rack structures using PSO, GWO, and IGWO algorithms. Adv. Struct Eng 2021;1369433221. https://doi.org/10.1177/13694332211004116.
[25] Kaveh A, editor. Advances in Metaheuristic Algorithms for Optimal Design of Structures. Cham: Springer International Publishing; 2014.
[26] Kaveh A, Talatahari S. Size optimization of space trusses using Big Bang-Big Crunch algorithm. Comput Struct 2009;87(17-18):1129–40. https://doi.org/10.1016/j.compstruc.2009.04.011.
[27] Camp CV, Farshchin M. Design of space trusses using modified teaching-learning based optimization. Eng Struct 2014;62–63:87–97. https://doi.org/10.1016/j.engstruct.2014.01.020.
[28] Kaveh A, Bakhshpoori T, Afshari E. An efficient hybrid Particle Swarm and Swallow Swarm Optimization algorithm. Comput Struct 2014;143:40–59. https://doi.org/10.1016/j.compstruc.2014.07.012.
[29] Kaveh A, Zakian P. Enhanced bat algorithm for optimal design of skeletal structures. Asian J Civ Eng 2014;15:179–212.
[30] Khatibinia M, Yazdani H. Accelerated multi-gravitational search algorithm for size optimization of truss structures. Swarm Evol Comput 2018;38:109–19. https://doi.org/10.1016/j.swevo.2017.07.001.
[31] Javidi A, Salajegheh E, Salajegheh J. Enhanced crow search algorithm for optimum design of structures. Appl Soft Comput J 2019;77:274–89. https://doi.org/10.1016/j.asoc.2019.01.026.
[32] Askari Q, Younas I, Saeed M. Political Optimizer: A novel socio-inspired meta-heuristic for global optimization. Knowledge-Based Syst 2020;195:105709. https://doi.org/10.1016/j.knosys.2020.105709.
[33] Diab AAZ, Tolba MA, El-Magd AGA, Zaky MM, El-Rifaie AM. Fuel cell parameters estimation via marine predators and political optimizers. IEEE Access 2020;8:166998–7018. https://doi.org/10.1109/Access.628763910.1109/ACCESS.2020.3021754.
[34] Yousri D, Abd Elaziz M, Oliva D, Abualigah L, Al-qaness MAA, Ewees AA. Reliable applied objective for identifying simple and detailed photovoltaic models using modern metaheuristics: Comparative study. Energy Convers Manag 2020;223:113279. https://doi.org/10.1016/j.enconman.2020.113279.
[35] Askari Q, Younas I. Political Optimizer Based Feedforward Neural Network for Classification and Function Approximation. Neural Process Lett 2021;53(1):429–58. https://doi.org/10.1007/s11063-020-10406-5.
[36] Jawad FKJ, Mahmood M, Wang D, AL-Azzawi O, AL-JAMELY A. Heuristic dragonfly algorithm for optimal design of truss structures with discrete variables. Structures 2021;29:843–62. https://doi.org/10.1016/j.istruc.2020.11.071.
[37] Degertekin SO. Improved harmony search algorithms for sizing optimization of truss structures. Comput Struct 2012;92–93:229–41. https://doi.org/10.1016/j.compstruc.2011.10.022.
[38] Kaveh A, Mirzaei B, Jafarvand A. An improved magnetic charged system search for optimization of truss structures with continuous and discrete variables. Appl Soft Comput J 2015;28:400–10. https://doi.org/10.1016/j.asoc.2014.11.056.
[39] Kaveh A, Zolghadr A. Cyclical Parthenogenesis Algorithm: A new meta-heuristic algorithm. Asian J Civ Eng 2017;18:673–701.
[40] Kaveh A, Akbari H, Hosseini SM. Plasma generation optimization: a new physically-based metaheuristic algorithm for solving constrained optimization problems. Eng Comput (Swansea, Wales) 2021;38(4):1554–606. https://doi.org/10.1108/EC-05-2020-0235.
[41] Imai K, Schmit LA. Configuration Optimization of Trusses. J Struct Div 1981;107(5):745–56. https://doi.org/10.1061/JSDEAG.0005702.
[42] SHEU CY, SCHMIT LA. Minimum weight design of elastic redundant trusses under multiple static loading conditions. AIAA J 1972;10(2):155–62. https://doi.org/10.2514/3.50078.
[43] Khan MR, Willmert KD, Thornton WA. An optimality criterion method for large-scale structures. AIAA J 1979;17(7):753–61. https://doi.org/10.2514/3.61214.
[44] Talatahari S, Kheirollahi M, Farahmandpour C, Gandomi AH. A multi-stage particle swarm for optimum design of truss structures. Neural Comput Appl 2013;23(5):1297–309. https://doi.org/10.1007/s00521-012-1072-5.
[45] Jalili S, Husseinzadeh Kashan A. An optics inspired optimization method for optimal design of truss structures. Struct Des Tall Spec Build 2019;28(6):e1598. https://doi.org/10.1002/tal.v28.610.1002/tal.1598.
[46] Jafari M, Salajegheh E, Salajegheh J. An efficient hybrid of elephant herding optimization and cultural algorithm for optimal design of trusses. Eng Comput 2019;35(3):781–801. https://doi.org/10.1007/s00366-018-0631-5.
[47] Kaveh A, Khayatazad M. Ray optimization for size and shape optimization of truss structures. Comput Struct 2013;117:82–94. https://doi.org/10.1016/j.compstruc.2012.12.010.
[48] Kaveh A, Ilchi GM. Enhanced colliding bodies optimization for design problems with continuous and discrete variables. Adv Eng Softw 2014;77:66–75. https://doi.org/10.1016/j.advengsoft.2014.08.003.
[49] Kaveh A, Zakian P. Improved GWO algorithm for optimal design of truss structures. Eng Comput 2018;34(4):685–707. https://doi.org/10.1007/s00366-017-0567-1.
[50] Ozbasaran H, Eryilmaz Yildirim M. Truss-sizing optimization attempts with CSA: a detailed evaluation. Soft Comput 2020;24(22):16775–801. https://doi.org/10.1007/s00500-020-04972-y.
[51] Dede T, Ayvaz Y. Combined size and shape optimization of structures with a new meta-heuristic algorithm. Appl Soft Comput J 2015;28:250–8. https://doi.org/10.1016/j.asoc.2014.12.007.
[52] Kaveh A, Talatahari S, Khodadadi N. Hybrid Invasive Weed Optimization-Shuffled Frog-Leaping Algorithm for Optimal Design of Truss Structures. Iran J Sci Technol - Trans Civ Eng 2020;44(2):405–20. https://doi.org/10.1007/s40996-019-00280-0.
[53] Toğan V, Daloğlu AT. An improved genetic algorithm with initial population strategy and self-adaptive member grouping. Comput Struct 2008;86(11-12):1204–18. https://doi.org/10.1016/j.compstruc.2007.11.006.
[54] Cao H, Qian X, Zhou Y. Large-scale structural optimization using metaheuristic algorithms with elitism and a filter strategy. Struct Multidiscip Optim 2018;57(2):799–814. https://doi.org/10.1007/s00158-017-1784-3.
[55] Hasancebi O, Erbatur F. On efficient use of simulated annealing in complex structural optimization problems. Acta Mech 2002;157(1-4):27–50. https://doi.org/10.1007/BF01182153.
[56] Hasançebi O. Adaptive evolution strategies in structural optimization: Enhancing their computational performance with applications to large-scale structures. Comput Struct 2008;86(1-2):119–32. https://doi.org/10.1016/j.compstruc.2007.05.012.
[57] Rahami H, Kaveh A, Aslani M, Najian AR. A hybrid modified genetic-nelder mead simplex algorithm for large-scale truss optimization. Int J Optim Civ Eng 2011;1:29–46.
[58] Gandomi AH, Talatahari S, Yang X-S, Deb S. Design optimization of truss structures using cuckoo search algorithm. Struct Des Tall Spec Build 2013;22(17):1330–49. https://doi.org/10.1002/tal.v22.1710.1002/tal.1033.
[59] Degertekin SO, Lamberti L, Ugur IB. Sizing, layout and topology design optimization of truss structures using the Jaya algorithm. Appl Soft Comput J 2018;70:903–28. https://doi.org/10.1016/j.asoc.2017.10.001.